



Originally published as:

Rodrigues Duran, E., di Primio, R., Anka, Z., Stoddart, D., Horsfield, B. (2013): Petroleum system analysis of the Hammerfest Basin (southwestern Barents Sea): comparison of basin modelling and geochemical data. - *Organic Geochemistry*, 63, p. 105-121.

DOI: <http://doi.org/10.1016/j.orggeochem.2013.07.011>

Accepted Manuscript

Petroleum system analysis of the Hammerfest Basin (southwestern Barents Sea): comparison of basin modelling and geochemical data

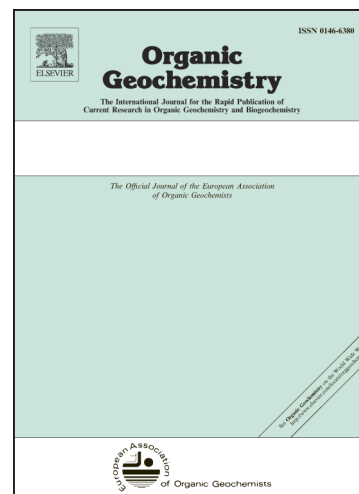
Enmanuel Rodrigues Duran, Rolando di Primio, Zahie Anka, Daniel Stoddart, Brian Horsfield

PII: S0146-6380(13)00162-9

DOI: <http://dx.doi.org/10.1016/j.orggeochem.2013.07.011>

Reference: OG 2985

To appear in: *Organic Geochemistry*



Please cite this article as: Duran, E.R., Primio, R.d., Anka, Z., Stoddart, D., Horsfield, B., Petroleum system analysis of the Hammerfest Basin (southwestern Barents Sea): comparison of basin modelling and geochemical data, *Organic Geochemistry* (2013), doi: <http://dx.doi.org/10.1016/j.orggeochem.2013.07.011>

This is a PDF file of an unedited manuscript that has been accepted for publication. As a service to our customers we are providing this early version of the manuscript. The manuscript will undergo copyediting, typesetting, and review of the resulting proof before it is published in its final form. Please note that during the production process errors may be discovered which could affect the content, and all legal disclaimers that apply to the journal pertain.

Petroleum system analysis of the Hammerfest Basin (southwestern Barents Sea): comparison of basin modelling and geochemical data.

Corresponding author: Rodrigues Duran, Enmanuel

The study was done at the German Research Centre for Geosciences (GFZ-Potsdam)

Current location

Statoil ASA

Mølnholtet 42

9414 Harstad-Norway

edur@statoil.com; erodrigues30@gmail.com

di Primio, Rolando

German Research Centre for Geosciences (GFZ-Potsdam)

Section 4.3-Organic Geochemistry

Telegrafenberg, House B

14473 Potsdam-Germany

Anka, Zahie

German Research Centre for Geosciences (GFZ-Potsdam)

Section 4.3-Organic Geochemistry

Telegrafenberg, House B

14473 Potsdam-Germany

Stoddart, Daniel

Lundin Norway AS

Strandveien 50 D

13366 Oslo-Norway

Horsfield, Brian

German Research Centre for Geosciences (GFZ-Potsdam)

Section 4.3-Organic Geochemistry

Telegrafenberg, House B

14473 PotsdamGermany

Petroleum system analysis of the Hammerfest Basin (southwestern Barents Sea): Comparison of basin modelling and geochemical data

**Enmanuel Rodrigues Duran, Rolando di Primio, Zahie Anka,
Daniel Stoddart, Brian Horsfield**

Abstract

Exploration in the Hammerfest Basin, southwestern Barents Sea, has proven several petroleum systems and plays with the presence of multiple source rocks of mainly Jurassic and Triassic age. To date several fields and discoveries have been found and are described to mainly contain gaseous hydrocarbons with the presence, in some cases, of an oil leg.

Our 3D Hammerfest Basin model shows that the Jurassic Hekkingen Formation and the Triassic Snadd and Kobbe formations reached high maturity levels (gas window) in the western and the northwestern margin. At the same time, this model reproduces the main hydrocarbon accumulations that have been found in the basin. An analysis of the volumetrics and the proportion of oil and gas contributions to each field and discovery, suggests that the gas contribution stems mainly from Triassic source rocks, while the oil phases contain variable proportions from the Jurassic Hekkingen Formation and Triassic source rocks.

Gas isotope and maturity related biomarker ratios confirm the maturity trends derived from the basin modelling results. Light hydrocarbons indicate the influence of secondary processes (biodegradation and long distance migration) in the petroleum from the Goliat field and the Tornerose discovery. Age related biomarker ratios such as the ETR (extended tricyclic terpane ratio) and the C_{28}/C_{29} steranes ratio did not provide a clear separation, when evaluating a contribution from Jurassic vs. Triassic source rocks.

1. Introduction

The Barents Sea has a complex geologic history extending from Palaeozoic to present day. In the last decades the area has been studied in detail in order to better understand this history (Vorren et al., 1991; Faleide et al., 1993; Johansen et al., 1993; Nøttvedt et al., 1993; Dimakis et al., 1998; Gudlaugsson et al., 1998; Ritzmann and Faleide, 2009). Special emphasis has been placed on the Cenozoic history since it was affected by several tectonic, paleoceanographic and paleoclimatic events that had a crucial influence on the hydrocarbon accumulation and distribution in the entire Barents Sea (Vorren et al., 1991; Linjordet and Grung-Olsen, 1992; Skagen, 1993; Doré and Jensen, 1996; Dimakis et al., 1998; Henriksen et al., 2011). Some of the major consequences related to these events are: (1) cessation of petroleum generation, expulsion and migration from the source rocks, 2) phase changes, including the expansion of gas in reservoir, which resulted in the spilling of earlier trapped oil, 3) reactivation of faults and breaching of seals associated to the reduction of overburden and pressure fluctuations, and 4) leakage of hydrocarbons from the reservoir to the surface, with the possible formation of gas hydrates and pockmarks (Larsen et

al., 1992; Chand et al., 2009; Chand et al., 2012; Ostanin et al., 2012, 2013; Rodrigues Duran et al., 2013).

The Barents Sea is characterized by the presence of multiple source rocks and hydrocarbon discoveries that consist mainly of underfilled gas fields, some of which have an oil leg (Ohm et al., 2008; Norwegian Petroleum Directorate, 2010b; Rodrigues Duran et al., 2013). Very few studies have been performed focusing on the geochemical correlation of the accumulated petroleum in order to define its possible origin. Johansen et al. (1993), Larsen et al. (1992), Linjordet and Grung-Olsen (1992), and Doré (1995) have identified the potential source rocks that could have contributed with petroleum to the main fields and discoveries in the Barents Sea. Ohm et al. (2008) carried out a geochemical analysis of the Norwegian Barents Sea fluids, in which they described the observations from geochemical analyses and defined the potential source rocks and the origin of petroleum accumulations in the Hammerfest Basin. Both Ohm et al. (2008) and He and Moldowan (2012), tried to decipher the types and distribution of source rocks in the Barents Sea and the Timan-Pechora Basin in Russia through the geochemical study of oil samples and an evaluation of the geographical extension of the source rocks. More recently, Rodrigues Duran et al. (2013) developed a 3D model of the Hammerfest Basin (southwestern Barents Sea) through which they reconstructed the present-day maturity of the three main source rocks proposed for this area, as well as the evolution of maturation through geologic time. In addition, petroleum migration, accumulation and leakage were modelled reproducing the present-day known accumulations with a large degree of accuracy. In this study we attempt to reconcile basin modelling

predictions and geochemical analytical results of oil and gas samples from the area in order to better understand the sources that contributed to the individual accumulations in the Hammerfest Basin; thus, improving our knowledge of the petroleum systems in this area.

2. Study area

The southwestern Barents Sea is characterized by several basins, highs and platforms, such as: the Hammerfest Basin, the Tromsø Basin, the Bjørnøya Basin, the Nordkapp Basin, the Loppa High, the Stappen High and the Finnmark and Bjarmeland Platforms (Fig. 1). Our study area covers mainly the Hammerfest Basin, in which the tectonic features observed today, were essentially created by Late Jurassic-Early Cretaceous faulting. Prior to, and also following, this faulting period the basin was part of a regional intracratonic basin (Berglund et al., 1986; Doré, 1995). The Hammerfest Basin is bounded to the south by the Troms-Finnmark Fault Complex, to the west by the Ringvassøy-Loppa Fault Complex, to the north by the Asterias Fault Complex and the Loppa High and to the east mainly by the Bjarmeland Platform (Fig. 1). This basin has been defined as one of the most important petroliferous basins in the southwestern Barents Sea, since the presence of several active petroleum systems has been proven by petroleum exploration (Larsen et al., 1992; Johansen et al., 1993; Doré, 1995).

3. Geologic history

Figure 2 summarizes the main stratigraphic units deposited in the Hammerfest basin and the major tectonic events that occurred in the area, as well as the most

important source rocks and the main reservoirs. The Barents Sea has a complex structural and sedimentary architecture as a result of several tectonic episodes, dominated by a long extension history since Devonian to Early Cenozoic time (Larsen et al., 1992; Faleide et al., 2008). Locally, minor compressional events were active, especially along the boundaries of major structural elements (Larsen et al., 1992). The Cenozoic history is characterized by large amounts of uplift and erosion in the basins and on structural highs, whereas at the shelf edge a thick wedge of Cenozoic sediments was deposited (Reemst et al., 1994). The important tectonic events associated with the opening of the North Atlantic, together with the stratigraphic relationships observed within the clastic wedges preserved in the Tertiary-Quaternary depocenters, illustrate the complex geologic history dominated by erosion. This erosion phase began in the Oligocene, after the maximum burial, and culminated during the Plio-Pleistocene glaciations (Nardin and Røssland, 1993). The geologic history in the Barents Sea has been already described by many authors and the reader is referred to these studies for more details (Berglund et al., 1986; Dalland et al., 1988; Dengo and Røssland, 1992; Larsen et al., 1992; Linjordet and Grung-Olsen, 1992; Johansen et al., 1993; Nøttvedt et al., 1993; Reemst et al., 1994; Doré, 1995; Gudlaugsson et al., 1998; O'Leary et al., 2004; Faleide et al., 2008; Ohm et al., 2008; Ritzmann and Faleide, 2009; Glørstad-Clark et al., 2010).

4. Petroleum plays in the southwestern Barents Sea

Data from exploration wells and from shallow boreholes have proven that potential reservoir and source rock sequences occur at several stratigraphic levels (Larsen et al., 1992; Ohm et al., 2008; Norwegian Petroleum Directorate, 2009,

2011). Larsen et al. (1992) documented that the Norwegian Barents Sea resources of 330 million Sm³ (standard cubic meter) oil equivalent have been proved by drilling, of which 90% correspond to gas and 85% is found in Lower–Middle Jurassic sandstones. The remainder is found in Lower Cretaceous and Lower and Upper Triassic sandstones. A summary of the most important petroleum plays that have been described for the Hammerfest Basin is shown in Table 1.

5. Materials and methods

5.1. Basin modelling

A 3D basin model of the Hammerfest Basin was built using the software PetroMod v.11 ® (Fig. 3). Details regarding model construction and calibration are described in Rodrigues Duran et al. (2013) and summarized here briefly. The model was defined using 16 structural maps provided by Lundin Norway AS, which were derived from seismic interpretation and represent the top or base of the main sedimentary sequences. The specific tops and bases used are: Base Ørret, Top Ørret, Base Kobbe, Top Kobbe, Top Snadd, Base Stø, Top Stø, Base Hekkingen, Top Hekkingen, Top Knurr, Top Kolje, Top Kolmule, Top Kveite, Base Quaternary and the Seabed (Table 2). The lithologic definition of each sequence (Table 2) was based on well data and on published work (Gabrielsen et al., 1990; Ohm et al., 2008). The well reports available in the Norwegian Petroleum Directorate website (Fact Pages) include the lithological description for every well. We used these descriptions in order to assign the lithologies in our model. Well data indicated only minor lateral and vertical variations in the sedimentary facies of each stratigraphic unit, with the exception of the main

reservoir (Stø Fm.), where a lateral facies occur and must have been considered in order to have a good approximation of the drainage areas and migration pathways.

For the petroleum system elements (Table 2) we considered three source rocks, two of Triassic age corresponding to the Snadd and Kobbe formations and one Jurassic, the Hekkingen Formation. The input values of total organic carbon (TOC) and hydrogen index (HI) for each source rock are reported in Table 2.

Since values were considered instead of maps, our model assumes a homogenous distribution of the same value over the entire study area. The main reservoir unit corresponds to the Jurassic Stø Formation, but also the Early Jurassic Tubåen Formation was assigned with reservoir properties. The seal in the Hammerfest Basin and for the Stø Formation in particular, consists mainly of the Fuglen Formation. Seal properties were evaluated and modified for the lithology of this unit in order to control the migration paths and to reproduce the accumulations. The traps present in the Barents Sea petroleum systems are of both, structural (rotated fault blocks and horsts) and stratigraphic types (pinch outs and halokinetic).

Two compositional kinetic models of petroleum generation and cracking were implemented for the Triassic (more type III kerogen) and the Jurassic (more type II kerogen) source rocks (Rodrigues Duran et al., 2013). These kinetic models use a 14 component scheme, which also includes secondary cracking (di Primio and Horsfield, 2006). The compositional kinetics were determined for samples of the main source rocks of the Barents Sea. Both the bulk kinetic and compositional

information were acquired combining open and closed system pyrolysis techniques. The compositional resolution covers the gas to heavy liquid range (C1, C2, C3, *i*-C4, *n*-C4, *i*-C5, *n*-C5, C6, C7-C15, C16-C25, C26-C35, C36-C45, C46-C55 and C55+), which allows the prediction of petroleum properties. The heavier components can be subjected to secondary cracking, and it is assumed that the only compound generated is methane.

Fluid flow was calculated using the hybrid migration routine of PetroMod, in which flow is calculated assuming Darcy flow in low permeability sequences and using flowpath analysis in high permeable carriers (Hantschel et al., 2000; Hantschel and Kauerauf, 2009; pages 286-287).

Boundary conditions, associated with the heat flow and the upper boundary of heat transfer, were assigned in the model through heat flow maps and a sediment water interface temperature trend, respectively. Seven heat flow maps were created and used to reproduce the evolution of the basin's thermal history. Three heat flow peaks associated with the rifting phases (140 and 65 Ma) and the regional subsidence (250 Ma) that took place in the Barents Sea were considered with higher heat flow values than the present day magnitude (58 mW/m²). A fourth heat flow increase is related to the maximum burial of the basin (Rodrigues Duran et al., 2013).

Calibration of the model was achieved using vitrinite reflectance (VR) and temperature (T) data available in the geochemical reports of the 24 wells assigned in the model. Information on the wells and the geochemical reports are

accessible in the FactPages of the NPD website (Norwegian Petroleum Directorate, 2009).

The scenario that allowed the best calibration to borehole T data corresponds to a background heat flow of 53–58 mW/m² (Rodrigues Duran et al., 2013). Two heat flow scenarios are suggested from the calibration to the VR data: a good calibration was achieved for some wells with a heat flow of 53–58 mW/m², while for other wells a lower present day heat flow of 45–50 mW/m² was required. In order to generate a basin model based on the best calibration results, we used a combination of both heat flow scenarios with regional variability (Rodrigues Duran et al., 2013).

The uplift and erosion of the Hammerfest Basin is mainly related to two regional events: (1) the structural development linked to the rifting, break-up, and subsequent opening of the Norwegian-Greenland Sea during the Oligocene-Miocene, and (2) the glacial activity during the Late Cenozoic (Berglund et al., 1986; Vorren et al., 1991; Nyland et al., 1992; Riis and Fjeldskaar, 1992; Knutsen et al., 1993; Richardsen et al., 1993; Riis, 1996; Dimakis et al., 1998; Cavanagh et al., 2006). These two erosion events were considered in the model, the first one from 30–15 Ma and the second one from 2.50–0.01 Ma. We used a similar erosional pattern for the two phases, but with a 2:1 magnitude relationship, with the Oligocene-Miocene being the larger one (Rodrigues Duran et al., 2013). The 3D modelling was performed in a deterministic manner, i.e. we carried out extensive sensitivity analyses considering possible heat flow history scenarios,

erosion scenarios and various glacial loading scenarios (Rodrigues Duran et al., 2013).

5.2. Geochemical data interpretation

The geochemical interpretation was performed on data kindly provided by Applied Petroleum Technology (APT) AS, Norway. APT is a well known service company that follows the NIGOGA analytical standards (Weiss et al., 2000). The available analytical data consisted of gas isotopes, gas and light hydrocarbon compositions, and biomarkers (steranes m/z 217 and 218; terpanes m/z 191; mono-aromatics steroids m/z 253; and tri-aromatic steroids m/z 231) from a total of 53 fluid samples representing the petroleum present in the main oil and gas accumulations of the study area. Detailed information regarding the sample types, the fields, and their stratigraphic level are described in Table 3. Additional well data for these samples cannot be given because they are proprietary.

6. Results

6.1. Basin modeling

6.1.1. Source rocks maturity

Figure 4 shows the present day maturation level and the maturation history of the three source rocks considered in the model, through the evolution of vitrinite reflectance. The maturation curves are presented for six pseudo-wells located in different areas of the basin: the northwestern margin and around the Snøhvit, Albatross, Askeladd and Goliat fields, as well as the Tornerose discovery (see locations in Fig. 4a). According to these results the three source rocks (Kobbe, Snadd and Hekkingen formations) reached high maturity levels mainly in the

western and the northwestern parts of the basin, with the Triassic Kobbe Formation reaching overmature or gas mature conditions in almost the entire basin. Assuming the onset of oil window maturity at ≈ 0.50 %VR (Tissot and Welte, 1984), the beginning of oil generation occurred from each source rock in the northwestern margin (where the highest maturity is observed) as follows: for the Kobbe Formation in the Late Triassic (~ 215 Ma), the Snadd Formation during the Early Cretaceous (~ 125 Ma), and the Hekkingen Formation in Late Cretaceous time (~ 100 Ma). The lowest maturity levels are found in the southeastern parts of the basin, around the Goliat field, where the Triassic Kobbe Formation would be the only source rock with an elevated maturity (early mature stage). The basin reached its maximum burial at 30 Ma (Fig. 5), followed by the uplift and erosion events previously mentioned in section 5.1. The onset of the Oligocene erosion in the Hammerfest Basin marks the end of hydrocarbon generation due to the cooling of the source rocks.

6.1.2. Hydrocarbon accumulations (main reservoir, Stø Formation)

The main hydrocarbon accumulations found to date in the Hammerfest Basin are accurately reproduced in our model (Fig. 6a). They correspond to Snøhvit, Snøhvit-Nord, Snøhvit-Beta, Albatross, Askeladd and Goliat fields and the Tornerose discovery. The first four fields consist mainly of natural gas with an oil leg, while the Askeladd field and the Tornerose discovery were reproduced as pure gas accumulations. The model predicts that the Goliat field as an accumulation dominated by oil with a small gas cap, which is in agreement with the information reported by the NPD (Norwegian Petroleum Directorate, 2010a). We emphasize that the combination of 14-component petroleum compositional

predictions with an equation of state based on PVT simulator correctly reproduced P/T influences on phase state, phase changes and phase properties of the modelled fluids.

As reported in the Norwegian Petroleum Directorate, the HCs found in the Snøhvit, Albatross and Askeladd fields are mainly present in the Stø Formation. In the Goliat field they are hosted in the Triassic Tubåen, Fruholmen, Snadd and Kobbe formations, and in the Tornerose discovery they are hosted in the Snadd and Stø formations. In our model, the petroleum accumulations have been reproduced mainly in the Stø Formation unit due to the lack of detailed maps for all relevant sedimentary units. However, as mentioned before, our model correctly reproduced the petroleum phases and properties in the modelled reservoirs, based on which we proceeded to perform the correlation of model results with the geochemical data interpretation.

The filling history of the Stø Formation (Fig. 6b) shows that petroleum (total oil and gas charged from the three source rocks: Hekkingen, Snadd and Kobbe formations) started to charge the reservoir from ~80 Ma until Oligocene time, when the main loss of oil occurred due to spilling out of the structures associated to the gas expansion and tilting that took place during the tectonic uplift. In the Pleistocene, the main loss of gaseous hydrocarbons is predicted to be associated to the glacial-interglacial cycles and concomitant erosion (Rodrigues Duran et al., 2013).

6.1.3. Prediction of hydrocarbon charge based on basin modelling

The possible provenance of the hydrocarbons in a modelled accumulation was evaluated by analyzing the hydrocarbon migration pathways and the drainage areas calculated by the 3D model (Fig. 7). The model results suggest that the Askeladd and Snøhvit fields were probably filled with hydrocarbons generated and expelled from the western and northern margins, respectively; while the Albatross field was charged from both areas. In the case of the Goliat field and the Tornerose discovery, the drainage areas and migration pathway analysis suggest that petroleum was probably generated mainly from the northern margin of the basin indicating a possible long distance migration.

An analysis of the volumetrics and the proportion of oil (liquid) and gas (vapor) contributions to each field and discovery as predicted by the basin model was also performed using source rock tracking, where generated components were tagged with information regarding which source rock generated them. Based on these results, we can also estimate the possible origin of the hydrocarbons present in reservoir (Table 4).

Accordingly, by combining the maturity results shown in Fig. 4 with the drainage areas, pathways and volumetrics analysis, it is possible to infer that the gas contribution in the Hammerfest Basin petroleum system was mainly from the Triassic Snadd and Kobbe formations (Table 4), with generation occurring in the western and northern areas, where the highest maturity levels (gas window, Fig. 4) were reached by these source rocks. In the case of the oil contribution, some differences were observed. For the Snøhvit field the main contributor was the Jurassic Hekkingen Formation, where the kitchen area is found mainly in the

north. For the Albatross and Goliat fields the modelling predicts (Table 4) that the main oil contribution was from the Triassic source rocks (mainly the Snadd Formation). In the case of the Albatross field the drainage areas suggest charging from the west and north, where the Snadd Formation is within oil window maturity (Figs. 4 and 7). The drainage areas associated to the Goliat field suggest, as previously mentioned, a contribution from the north, where once again the Snadd Formation is within the oil window. On the other hand, when looking at the filling history of this particular field (Fig. 8), we observed that the main filling pulse occurred after 30 Ma, i.e. after the tectonic uplift of the basin. Therefore, we infer that a portion of the petroleum in this field stems from spilling from as far as the Snøhvit field in the northern margin, indicating the possibility of long distance migration contributing to the charge (Rodrigues Duran et al., 2013). A local contribution from the Kobbe Formation should also be considered for this particular field, whereby vertical migration is suggested since maturity levels within the oil window were reached by this source rock in the area. The hydrocarbon migration vectors observed in the model indicate that in the Goliat area, petroleum could have migrated vertically from the source rock and into the reservoir unit.

6.2. Gas isotopes

Analysis of gas isotopes and composition allows differentiating sources of gas, alteration mechanisms and maturity. We applied some established interpretation schemes (Bernard et al., 1978; Tissot and Welte, 1984; Berner and Faber, 1988; Whiticar, 1994; Berner and Faber, 1996; Whiticar, 1996; Aali et al., 2006) for these investigations, the results of which are shown in Figs. 9 and 10.

Figure 9a shows a correlation between the $\delta^{13}\text{C}$ of methane and gas dryness, defined as the proportion of methane in relation to ethane and propane or $\text{C}_1/(\text{C}_2+\text{C}_3)$ (Bernard et al., 1978). Figure 9b shows a correlation of methane isotopic composition using the wetness percentage, defined as the proportion of C_2-C_4 hydrocarbons in the total C_1-C_4 gas mixture (Tissot and Welte, 1984). Both plots show that all accumulated gases have a dominantly thermogenic origin. They demonstrate that some samples from the Goliat field, present in the Tubåen and Snadd formations (shallow depths), are in the area of mixed microbial-thermogenic gas, which indicates possible biodegradation as reported by Ohm et al. (2008) and the NPD (Norwegian Petroleum Directorate, 2010a). Alternatively, it is possible to deduce from Fig. 9b that all the samples can be defined as associated gas. The samples from Askeladd, as well as some samples from Snøhvit, Albatross and Goliat (Tubåen and Snadd formations) fields and the Tornerose (Snadd Formation) discovery are mainly condensate associated, while other samples from the Snøhvit, Albatross and Goliat (Kobbe Formation) fields and the Tornerose (Stø Formation) discovery are oil associated. The basin modelling results do not give information that allow us to make a correlation with the previous interpretation regarding oil or condensate associated gas origin. However, based on the petroleum phases predicted for each field in the model we can assume that in the case of Snøhvit, Albatross and Goliat fields where oil and gas columns have been predicted to occur, we could expect the dominance of an oil associated gas. The Askeladd field and the Tornerose discovery were reproduced as pure gas fields, indicating that higher maturity fluids, i.e. condensate associated gas, should dominate there.

Figure 10a-c shows gas isotopic correlations of ethane vs. propane and methane vs. ethane, as well as an interpretation of the possible maturity level of the samples assuming, in some cases (Fig. 10a, b), specific types of kerogen. The isotopically lightest sample and also the one presenting the lowest maturity ($\sim 0.70\%$ VR) is found in the Tornerose discovery within the Stø Formation unit (Fig. 10a). This is in accordance with the model results since maturity levels around this value have been reached by the Snadd and Hekkingen formations in the area (Fig. 4). Samples from Snøhvit and Albatross fields, as well as some samples from Goliat field and the Tornerose discovery show a maturity level between 0.85% VR and 1.30% VR (early mature or oil window to gas mature). The samples from the Askeladd field show the highest maturity level ($1.30\text{--}1.80\%$ VR). Once again these observations correlate with the modeling results, as the highest maturity levels from both the Kobbe and Snadd formations were reached in the western areas from where the Askeladd field has been filled.

6.3. Light hydrocarbons analysis and interpretation

We used the light hydrocarbons (C_7) compositional data, in order to correlate samples in the different fields. The possible influence of secondary processes, such as biodegradation, water washing, TSR (thermochemical sulfate reduction) and evaporative fractionation were evaluated using the Halpern (1995) and Thompson (1983) parameters. The Halpern parameters are plotted on two star diagrams, corresponding to the C_7 oil correlation and C_7 oil transformation diagrams (Fig. 11). The C_7 oil correlation diagram (Fig. 11) shows that all the samples have a similar pattern, indicating similar sources for the fluids.

However, the C_7 oil transformation diagram (Fig. 11) indicates some differences mainly related to the samples from Goliat field. The ratios in this plot, with the exception of the Tr1 and Tr6, are especially sensitive to biodegradation.

Accordingly, variability among these samples from the Goliat field can be attributed to biodegradation as already described by Ohm et al. (2008). The Tr1 and Tr6 ratios indicate the loss of water soluble aromatic compounds, which can be used to suggest long distance migration. Once again samples in the Goliat field show differences in these two ratios and also samples from the Tornerose discovery show a slight decrease in Tr1. For these two accumulations long distance migration of petroleum appears likely and is supported by the basin modelling results, as discussed earlier (Fig. 7d, e).

A star diagram of the Thompson parameters is shown for each field in Figure 12. These parameters show a large degree of similarity for the samples in Snøhvit, Albatross and Askeladd fields and the Tornerose discovery. Samples from the shallower parts of the Goliat field (Tubåen and Snadd formations) show a clear signature of biodegradation. The deepest samples in the Goliat field (Kobbe Formation) are similar to the samples in the other fields, but the slight variability discernible can be used to suggest the possibility of a different oil source. Additionally, differences in some parameters such as Thompson F and S can also be used to indicate a modest water washing and therefore long distance migration.

Figure 13 shows a cross plot of the heptane and isoheptane indices (Thompson, 1983) which allows the assessment of source, maturity and alteration effects. The

figure show that the samples from the Snøhvit, Albatross and Askeladd fields plot close together in the mature zone of the diagram and close to the type II kerogen curve (or aliphatic curve) based on the Thompson (1983) interpretation. The trend from Snøhvit to Albatross tentatively indicates a maturity trend (also supported by the gas isotopes), whereas the Askeladd field data extends into areas with higher maturity and is as well shifted towards the type III kerogen trend line. Samples from a well in the Southern Loppa High Fault Complex (SLHFC) are located close to the type II curve, and show a comparatively lower maturity for samples from the Hekkingen Formation and higher maturity for samples from the Knurr Formation. Samples from the Tornerose discovery plot close to the type III kerogen curve (or aromatic curve) indicating the likelihood of a different source contributing here than in the western Hammerfest Basin fields. Alternatively, the Tornerose hydrocarbon composition may also have been slightly influenced by biodegradation resulting in a shift of the original composition towards lower heptane and isoheptane ratios. However no signs of biodegradation were obvious in the gas isotopes and the light hydrocarbons. Finally, samples from the Goliat field have low heptane and iso-heptane ratios, and therefore plot in the biodegradation zone, corroborating previous results and information from well reports (Ohm et al., 2008; Norwegian Petroleum Directorate, 2010a).

6.4. Paleo-environment interpretation

Figure 14a shows the correlation of pristane/ n -C₁₇ versus phytane/ n -C₁₈ and indicates that all the samples are in the early mature stage and have been predominantly derived from a similar type of organic matter. Only the samples

from Askeladd field are slightly shifted towards a more oxic depositional environment supporting the trend observed in the light hydrocarbon analysis (Fig. 13). The fact that the samples in the Tornerose discovery plot in the same area as Snøhvit, Albatross and Goliat may point towards similar source rock types, supporting as well the interpretation that differences in the light hydrocarbon composition (Fig. 13) are only the result of biodegradation.

On the other hand, Fig. 14b-c targets the depositional environment of the source rocks that generated the oils accumulated in the area. A marine environment is suggested for all samples. However, based on the sterane distribution diagram (Fig. 14b) it is obvious that samples from Goliat field (in the Kobbe, Snadd and Tubåen formations) and Tornerose discovery (in the Snadd Formation) plot close together, and distinctly separate from the Snøhvit, Albatross and Askeladd group, in the area characteristic for shallow marine or coastal environment. This could also be an indication of biodegradation which produces a selective depletion in the C₂₇ steranes (Peters et al., 2005; p. 674). However, the level of biodegradation required to affect the steranes has not been reported for any of the fields studied. Accordingly the variability in the steranes distribution most likely reflects the sourcing from the same general type of source rock but with variations of organic facies. Figure 14c indicates only minor facies variability in the sample set.

6.5. Maturity-related biomarkers

Figure 15 shows star diagrams with seven maturity ratios determined from selected steranes, terpanes and aromatic steroids. In the case of the Snøhvit,

Albatross and Askeladd fields two similar trends can be recognized (Fig. 15a-c), which may reflect two different oil families with different maturity levels or different source rocks. For the Goliat field and the Tornerose discovery there are also two trends, which at the same time differ from the two trends observed in the Snøhvit, Albatross and Askeladd fields. The $22S/(22S+22R)$ C_{32} homohopane as well as the $20S/(20S+20R)$ C_{29} sterane ratios show full isomerization in all cases. The main differences are observed in the $Ts/(Ts + Tm)$, the diasteranes/steranes, and the C_{29} iso/regular steranes and the ratios, the three of them are not only maturity sensitive but respond also to facies variations. The $Ts/(Ts + Tm)$ is most reliable as a maturity indicator when evaluating oils from a common source of consistent organic facies (Peters et al., 2005; p. 616). One group of samples shows higher Ts/Tm and C_{29} iso/regular steranes ratios associated to lower diasterane/sterane ratios (Snøhvit West and Nord, Albatross NW, Askeladd East and West, and Tornerose in the Snadd and Stø formations), while a second group of samples shows elevated diasteranes/steranes ratios associated to lower $Ts/(Ts+Tm)$ and C_{29} iso/regular steranes ratios values (Snøhvit West, Central and Beta, Albatross NE, Askeladd East, central and West, and Tornerose in the Snadd Formation). Tentatively, these groups of fluids could be attributed to be products of different source rocks that reached different maturity levels. A clear representation of the samples distribution for the first two ratios is shown in Fig. 16.

According to this cross plot, samples from Goliat in the Kobbe Formation plot are separated from the rest indicating a likely contribution from a different source rock. For this particular case we could tentatively postulate that the

hydrocarbons were generated from the same sequence in which they were found (Kobbe Formation), since as mentioned before, this source rock reached oil window maturity levels in the southwestern margin around the Goliat field. On the other hand, the variability among the other two groups that occurs within the individual fields could certainly indicate facies differences, generation from different rocks, mixing of hydrocarbons in the reservoirs and different maturity levels.

With respect to maturity, the aromatic steroid (MAS and TAS) and the C₂₉ iso/regular steranes ratios are the only measured maturity indicators applicable to the late oil window and suggest maturity levels of 0.7–0.8 %VR for almost all the fields with the exception of Goliat (Fig. 15f, Peters et al., 2005). In the Goliat field these ratios suggest lower maturity levels, i.e. of 0.6–0.7 %VR.

6.6. Age-related biomarkers

Based on the assumption that most of the petroleum in the Hammerfest Basin has been predominantly sourced by the Jurassic Hekkingen Formation and the Triassic Snadd and Kobbe formations, we used the extended tricyclic terpane ratio (ETR, Holba et al., 2001) and the C₂₈/C₂₉ steranes ratio (Grantham and Wakefield, 1988) as age diagnostic biomarkers to address contributions from source rocks of these ages.

The ETR $((C_{28} + C_{29})/(C_{28} + C_{29} + Ts))$ defined by Holba et al. (2001) can be used to differentiate crude oils (within the oil window) generated from Triassic, Lower Jurassic and Middle-Upper Jurassic source rocks. The study made by Holba et al.

(2001) using a worldwide crude oil sample dataset shows that the Triassic oil samples have ETRs ≥ 2.0 ; Early Jurassic oil samples have ETRs ≤ 2.0 ; and Middle or Late Jurassic oil samples have ETRs ≤ 2.0 , with most of the samples being < 1.2 . In our dataset we observe that all the values for this ratio in the Hammerfest Basin are below 1.2.

The C_{28}/C_{29} steranes ratio is also an age related parameter used for oils lacking terrigenous input. Grantham and Wakefield (1988), evaluated the variations in the sterane carbon number distribution (from C_{27} to C_{29}) of crude oils derived from marine source rocks in correlation with the time at which the source rocks were deposited. They observed that the relative proportions of C_{27} steranes show no particular trends through geological time, while the C_{28} steranes show a clear trend of increasing percentages through time and the C_{29} steranes show a broad trend of decreasing percentages through geological time. Grantham and Wakefield (1988) combined the percentages of C_{28} and C_{29} steranes as a ratio and plotted this ratio against the geological age of the source rocks. The results show that the ratio is < 0.5 for Lower Palaeozoic and older oils, values between 0.4 and 0.7 are observed for oils from Upper Paleozoic to Lower Jurassic and for Upper Jurassic to Miocene oils the values are greater than ~ 0.7 .

Figure 17 shows the samples from the Snøhvit and Goliat fields, the Tornerose discovery and the well located in the SLHFC plotting in an interval from 0.5 to 0.9 (C_{28}/C_{29} sterane ratio), indicating a highly variable source age extending from Triassic to Upper Jurassic, which means that a clear source differentiation based only on age related biomarkers is not possible. However, the general trend in

which the samples plot indicates that some Snøhvit and Tornerose oils are likely sourced from the Upper Jurassic Hekkingen Formation, while most other fluids show a tendency for contributions from older, probably Triassic, source rocks.

7. Discussion

7.1. Correlation of organic geochemistry data and basin modelling

The deconvolution of petroleum sources in a setting characterized by multiple source rocks and reservoirs, single and two phase accumulations, a complex geologic history as well as variable analytical coverage of the available samples make a conclusive interpretation difficult. This is especially true in the comparison of interpretations based on analysis of different compound ranges, e.g. gases, light hydrocarbons and the liquid fraction. The comparison of geochemical interpretations regarding source rocks contributing to individual reservoirs, with results derived from the numerical simulation of basin evolution (which includes source rock maturation, petroleum generation, migration, accumulation and leakage), requires consideration of the scales for which analytical or modelling results apply. While geochemical analysis gives information on samples representative for an individual carrier in a reservoir, modelling of petroleum charge of the same reservoir provides results at the resolution of the entire field. Nevertheless, both data types can be integrated and compared, albeit at a coarser level than is usual for geochemical data. In the following we will focus on discussing general regional observations regarding the contributions from different source rocks, their regional variability and the types of fluids generated.

Both basin modelling and geochemical data indicate that the hydrocarbons present in the main accumulations of the Hammerfest Basin represent mixture of hydrocarbons generated and expelled from both Triassic and Jurassic source rocks. This general conclusion is in accordance with the results reported by Ohm et al. (2008), who argued that the isotopically heavy values of oil fractions ($> 29\%$) in most of the Hammerfest Basin oils is an indication of the mixing of Hekkingen derived oils with pre-Jurassic oils (Triassic and even Paleozoic oils). Considering the complex geologic history of the basin, especially during the Cenozoic, makes clear that a mixing of hydrocarbons after they have reached the reservoir structure is possible.

Gaseous hydrocarbons present in Askeladd were probably charged from the Triassic Snadd and Kobbe formations, since gas isotopes suggest for this field the highest maturity levels of 1.3–1.5 %VR (Fig. 10). Model results show that the drainage areas for this field are linked to the western margin of the basin where VR values of this magnitude and even higher were reached by the respective source rocks (Fig. 4). Mass balances from the basin modelling (Table 4) also report that the main contribution was from the Triassic source rocks, mainly the Snadd Formation. Charges from these two formations can also be supported by the maturity related biomarkers (Fig. 15), which show the presence of hydrocarbons with two maturity tendencies. However, it should be kept in mind that the ratios that indicate the highest maturity are the diasteranes/sterane and the $T_s/(T_s+T_m)$, and as already mentioned, these ratios are not exclusively indicators of maturity. It is important to note that the Kobbe and Snadd formations generated oil during early maturation. This oil is predicted to

accumulate in the Askeladd, Albatross and Snøhvit fields during Late Cretaceous time. Later on (Early Paleocene) with the increasing of maturity, the gas generated and expelled started to accumulate as well in the reservoirs, resulting in the displacement of oil out of these structures.

According to the gas isotopic compositions, the Snøhvit and Albatross fields show lower maturity levels (0.85–1.30 %VR) indicating that these fields have probably been mainly charged by hydrocarbons from the Jurassic Hekkingen Formation, as this maturity stage is observed for this source rock in the northern margin (Fig. 4); whereas the Kobbe and Snadd formations are overmature (VR > 1.50%) in this area. Gas isotopic compositions also suggest that these two fields contain condensate- and oil- associated gas. This is in accordance with the well data (Norwegian Petroleum Directorate, 2009) and with the results from 3D modelling (Rodrigues Duran et al., 2013), where the Snøhvit field is characterized as an oil rimmed gas accumulation. Biomarker parameters (Fig. 15) also suggest two maturity tendencies. The contribution from both sources (Triassic and Jurassic source rocks) is suggested by the mass contribution obtained from the model and reported in Table 4. Ohm et al. (2008) studied some oils from the Snøhvit field and suggested that they are probably the result of petroleum mixing from different sources, even from deeper Paleozoic source rocks.

In the case of the Goliat field and the Tornerose discovery, maturity levels of 0.70–1.30 %VR are inferred from the gas isotopic composition (Section 6.3).

Looking at the regional source rock maturities of the 3D model (Fig. 4), generation from a local source and subsequent vertical migration can only be

suggested to have occurred from the Triassic Kobbe and Snadd formations, because only these two source rocks reached oil window maturity levels in the areas where the accumulations are located and, in fact, the accumulations in the Goliat field are found within Triassic intervals (Norwegian Petroleum Directorate, 2010a). However, as discussed above, a charging from the northern margin is suggested by the modelled flow paths and drainage areas (Fig. 7). Modelling in this case suggests the possibility of long distance migration from the north and thus a possible contribution from the Jurassic Hekkingen Formation.

Two trends in maturity related biomarkers are observed in the Goliat field and the Tornerose discovery (Fig. 15). In the case of Goliat field the two different groups observed could be attributed to the shallower oil being biodegraded, as discussed earlier, and not due to the presence of two different petroleum families coming from two different sources with different maturities. However, we cannot exclude either possibility, i.e. less mature petroleum sourced from Hekkingen Formation and migrating long distances or petroleum sourced from the higher maturity Triassic sequences, mainly the Kobbe Formation, which could also have contributed to the gaseous hydrocarbons found in the field (Rodrigues Duran et al., 2013). This dual contribution is visible in the modelling results (Table 4), which indicate that the liquid phase in the Goliat field has been received charges in equal proportions from both sequences, Jurassic and Triassic. Ohm et al.

(2008) also performed a detail analysis of the oils in the Goliat field and suggested that these oils represent a mixing of Triassic and Jurassic oil based on the *n*-alkane profiles and the isotopic values of the saturated oil fraction. The isotopic data available for our study are the same data used by Ohm et al. (2008).

On the other hand, two maturity levels are also observed for the hydrocarbons in the Tornerose discovery, one 0.85–1.30 %VR (according to the gas isotopic composition, Fig. 10) and the second 0.70–0.80 %VR (gas isotopes and maturity related biomarkers, Figs. 10 and 15). The flow path and drainage area analysis from the model results indicate that hydrocarbons present in this discovery originated from the northern areas. Therefore, petroleum could have been generated from the Jurassic Hekkingen Formation or even from the Triassic Snadd Formation, which reached these maturity levels in the northern margin. Modelling results correctly suggest that the accumulation consist mainly of gas (Rodrigues Duran et al., 2013) with a main contribution from the Triassic Kobbe and Snadd formations (Table 4).

The age related biomarkers did not show a clear tendency with respect to the origin of the hydrocarbons. The C_{28}/C_{29} steranes ratio suggests that the hydrocarbons present in the fields and discoveries (Fig. 17) are a mixture, sourced from both the Triassic and Jurassic source rocks. For the particular case of the Tornerose discovery two groups are observed, one suggesting an Upper Jurassic origin, i.e. hydrocarbons being generated from the Hekkingen Formation, and the second one suggesting a Lower Jurassic or Triassic origin, i.e. hydrocarbons being generated from the Snadd and Kobbe formations. A Jurassic origin is suggested from the ETR, which indicates that all the hydrocarbon samples should have been derived from a Jurassic source rock (Hekkingen Formation). However, Ohm et al. (2008) found values of ETR from two Triassic source rock extracts from the well 7120/2-1 (southern part of the Loppa High) to

be around zero and they argued that the low ETR is a result of low maturity. Additionally, Ohm et al. (2008) also observed that the ETRs of oils in the Triassic Snadd and Kobbe formations of the Goliat field are less than 2, suggesting that they should be of Jurassic origin. Therefore, these values together with the values of ETR below 2 from the Triassic extracts indicate that low ETR values do not always support a Jurassic origin. Ohm et al. (2008) also compared the *n*-alkane distribution of the Snadd and Kobbe formations oils from Goliat with Triassic oils from the Sverdrup Basin and Alaska, and observed a very good match, suggesting that Goliat oils could have a Triassic origin regardless of the low ETR.

The integration of 3D petroleum system modelling with geochemical data, results in a relatively good match of predictions and observations, especially with respect to maturity of the oils and their respective kitchen areas, and provides indications of the processes controlling the observed variability. We inferred long range migration, biodegradation and petroleum mixing stand out as the main processes that result from the complex geologic history of the basin and make it difficult to pinpoint specific source rock contributions, i.e. Triassic vs. Jurassic.

8. Conclusions

Integration of the results presented in this work allows developing a better understanding of the possible contributions from individual source rocks to the petroleum accumulations of the Hammerfest Basin. Basin modelling indicates that high maturity levels have been reached in the western and northwestern margin of the basin by the Kobbe, Snadd and Hekkingen source rocks. These

results also indicate that the main gas charge was from the Triassic source rocks, while the oil charges were from both the Jurassic Hekkingen Formation and the Triassic Snadd and Kobbe formations. The modelled drainage areas suggest a relatively local source from the west and north to the Askeladd, Albatross and Snøhvit fields, while a combination of a local source contribution as well as long distance migration can be proposed for the Goliat field and the Tornerose discovery.

The organic geochemical data interpretation supports in general the results from basin modelling. However, age related biomarkers suggest that hydrocarbons present in the main accumulations of the Hammerfest Basin do not have a clear tendency regarding their origin from Triassic or Jurassic source rocks. Gas analysis also indicates a maturity gradient from west to east. Light hydrocarbons support long range migration routes to Tornerose and Goliat, and also support the biodegradation of the oils in the Goliat field. Finally biomarkers indicate the likely contribution of two source rock facies types to the liquid fraction of the petroleum accumulations hosted in the Hammerfest Basin. Our work indicates that the integration of basin modelling predictions and geochemical data is a powerful combination that enhances the understanding of the processes controlling basin, source rock and petroleum accumulation evolution.

Acknowledgments

The authors thank Lundin Norway AS for providing the surface maps used in the model building. Thanks are due to Nigel Mills and APT Norway for providing access to the geochemical data. This work is also a contribution to the Helmholtz

Climate Initiative REKLIM (Regional Climate Change), a joint research project of the Helmholtz Association of German research centres (HGF). Zahie Anka is head of a Helmholtz-University Young Investigator Group funded by the Helmholtz Association's Initiative and Networking Fund. The authors also would like to thank Chris Cornford and an anonymous reviewer for their comments and suggestions.

Associate Editor – **Cliff Walters**

References

- Aali, J., Rahimpour-Bonab, H., Kamali, M.R., 2006. Geochemistry and origin of the world's largest gas field from Persian Gulf, Iran. *Journal of Petroleum Science and Engineering* 50, 161-175.
- Berglund, L.T., Augustson, J., Færseth, R., Gjelberg, J., Ramberg-Moe, H., 1986. The evolution of the Hammerfest Basin. In: Spencer, A.M., Holter, E., Campbell, C.J., Hanslien, S.H., Nelson, P.H.H., Nysæther, E., Ormaasen, E.G. (Eds.), *Habitat of Hydrocarbons on the Norwegian Continental Shelf*. Graham & Trotman, London, pp. 319-338.
- Bernard, B.B., Brooks, J.M., Sackett, W.M., 1978. Light hydrocarbons in recent Texas continental shelf and slope sediments. *Journal of Geophysical Research* 83, 4053-4061.
- Berner, U., Faber, E., 1988. Maturity related mixing model for methane, ethane and propane, based on carbon isotopes. *Organic Geochemistry* 13, 67-72.

- Berner, U., Faber, E., 1996. Empirical carbon isotope/maturity relationships for gases from algal kerogens and terrigenous organic matter, based on dry, open-system pyrolysis. *Organic Geochemistry* 24, 947-955.
- Cavanagh, A.J., di Primio, R., Scheck-Wenderoth, M., Horsfield, B., 2006. Severity and timing of Cenozoic exhumation in the southwestern Barents Sea. *Journal of the Geological Society* 163, 761-774.
- Chand, S., Rise, L., Ottesen, D., Dolan, M.F.J., Bellec, V., Bøe, R., 2009. Pockmark-like depressions near the Goliat hydrocarbon field, Barents Sea: Morphology and genesis. *Marine and Petroleum Geology* 26, 1035-1042.
- Chand, S., Thorsnes, T., Rise, L., Brunstad, H., Stoddart, D., Bøe, R., Lågstad, P., Svolsbru, T., 2012. Multiple episodes of fluid flow in the SW Barents Sea (Loppa High) evidenced by gas flares, pockmarks and gas hydrate accumulation. *Earth and Planetary Science Letters* 331–332, 305-314.
- Dalland, A., Worsley, D., Ofstad, K., 1988. A lithostratigraphic scheme for the Mesozoic and Cenozoic succession offshore mid- and northern Norway. *Norwegian Petroleum Directorate Bulletin* 4, 1-65.
- Dengo, C.A., Røssland, K.G., 1992. Extensional tectonic history of the western Barents Sea. In: Larsen, R.M., Brekke, H., Larsen, B.T., Talleraas, E. (Eds.), *Structural and Tectonic Modelling and its Application to Petroleum Geology*. Norwegian Petroleum Society, Special Publication 1, pp. 91-107.

- di Primio, R., Horsfield, B., 2006. From petroleum-type organofacies to hydrocarbon phase prediction. *American Association of Petroleum Geologists Bulletin* 90, 1031-1058.
- Dimakis, P., Braathen, B.I., Faleide, J.I., Elverhøi, A., Gudlaugsson, S.T., 1998. Cenozoic erosion and the preglacial uplift of the Svalbard-Barents Sea region. *Tectonophysics* 300, 311-327.
- Doré, A.G., 1995. Barents Sea geology, petroleum resources and commercial potential. *Arctic* 48, 207-221.
- Doré, A.G., Jensen, L.N., 1996. The impact of late Cenozoic uplift and erosion on hydrocarbon exploration: Offshore Norway and some other uplifted basins. *Global and Planetary Change* 12, 415-436.
- Faleide, J.I., Tsikalas, F., Breivik, A.J., Mjelde, R., Ritzmann, O., Engen, Ø., Wilson, J., Eldholm, O., 2008. Structure and evolution of the continental margin off Norway and the Barents Sea. *Episodes* 31, 82-91.
- Faleide, J.I., Vågnes, E., Gudlaugsson, S.T., 1993. Late Mesozoic-Cenozoic evolution of the south-western Barents Sea in a regional rift-shear tectonic setting. *Marine and Petroleum Geology* 10, 186-214.
- Gabrielsen, R.H., Færseth, R.B., Jensen, L.N., Kalheim, J.E., Riis, F., 1990. Structural elements of the Norwegian continental shelf. Part I: The Barents Sea Region. *Norwegian Petroleum Directorate Bulletin* 6, 1-47.

- Glørstad-Clark, E., Faleide, J.I., Lundschieen, B.A., Nystuen, J.P., 2010. Triassic seismic sequence stratigraphy and paleogeography of the western Barents Sea area. *Marine and Petroleum Geology* 27, 1448-1475.
- Grantham, P.J., Wakefield, L.L., 1988. Variations in the sterane carbon number distributions of marine source rock derived crude oils through geological time. *Organic Geochemistry* 12, 61-73.
- Gudlaugsson, S.T., Faleide, J.I., Johansen, S.E., Breivik, A.J., 1998. Late Palaeozoic structural development of the South-western Barents Sea. *Marine and Petroleum Geology* 15, 73-102.
- Halpern, H.I., 1995. Development and applications of light-hydrocarbon-based star diagrams. *American Association of Petroleum Geologists Bulletin* 79, 801-815.
- Hantschel, T., Kauerauf, A.I., 2009. *Fundamentals of Basin and Petroleum Systems Modelling*. Springer-Verlag, Berlin, Heidelberg.
- Hantschel, T., Kauerauf, A.I., Wygrala, B., 2000. Finite element analysis and ray tracing modeling of petroleum migration. *Marine and Petroleum Geology* 17, 815-820.
- He, M., Moldowan, J.M., 2012. Oil families and their inferred source rocks in the Barents Sea and northern Timan-Pechora Basin, Russia. *American Association of Petroleum Geologists Bulletin* 96, 1121-1146.
- Henriksen, E., Bjørnseth, H.M., Hals, T.K., Heide, T., Kiryukhina, T., Kløvjan, O.S., Larssen, G.B., Ryseth, A.E., Rønning, K., Sollid, K., Stoupakova, A.,

2011. Uplift and erosion of the greater Barents Sea: Impact on prospectivity and petroleum systems. In: Spencer, A.M., Embry, A.F., Gautier, D.L., Stoupakova, A.V., Sørensen, K. (Eds.), Arctic Petroleum Geology. Geological Society of London, London, pp. 271-281.
- Holba, A.G., Ellis, L., Dzou, I.L., Hallam, A., Masterson, W.D., Francu, J., Fincannon, A.L., 2001. Extended tricyclic terpanes as age discriminators between Triassic, Early Jurassic, and Middle–Late Jurassic oils. (abs.): 20th International Meeting on Organic Geochemistry, September 10–14, 2001, Nancy-France, v. 1, p. 464.
- Johansen, S.E., Ostistiy, B.K., Birkeland, Ø., Fedorovsky, Y.F., Martirosjan, V.N., Bruun Christensen, O., Cheredeev, S.I., Ignatenko, E.A., Margulis, L.S., 1993. Hydrocarbon potential in the Barents Sea region: play distribution and Potential. In: Vorren, T.O., Bergsager, E., Dahl-Stamnes, Ø.A., Holter, E., Johansen, B., Lie, E., Lund, T.B. (Eds.), Arctic Geology and Petroleum Potential. Norwegian Petroleum Society, Special Publication 2, pp. 273-320.
- Knutsen, S.-M., Richardsen, G., Vorren, T.O., 1993. Late Miocene-Pleistocene sequence stratigraphy and mass-movements on the western Barents Sea margin. In: Vorren, T.O., Bergsager, E., Dahl-Stamnes, Ø.A., Holter, E., Johansen, B., Lie, E., Lund, T.B. (Eds.), Arctic Geology and Petroleum Potential. Norwegian Petroleum Society, Special Publication, pp. 573-606.
- Larsen, R.M., Fjæran, T., Skarpnes, O., 1992. Hydrocarbon potential of the Norwegian Barents Sea based on recent well results. In: Vorren, T.O., Bergsager, E., Dahl-Stamnes, Ø.A., Holter, E., Johansen, B., Lie, E., Lund,

T.B. (Eds.), Arctic Geology and Petroleum Potential. Norwegian Petroleum Society, Special Publication 2, pp. 321-331.

Linjordet, A., Grung-Olsen, R., 1992. The Jurassic Snøhvit Gas Field, Hammerfest Basin, offshore northern Norway. American Association of Petroleum Geologists Memoir 54, 349-370.

Nardin, T.R., Røssland, K.G., 1993. Restoration of the eroded section in the western Barents Sea. In: Vorren, T.O., Bergsager, E., Dahl-Stammes, Ø.A., Holter, E., Johansen, B., Lie, E., Lund, T.B. (Eds.), Arctic Geology and Petroleum Potential. Norwegian Petroleum Society, Special Publication 2, pp. 607-618.

Norwegian Petroleum Directorate, 2009. The Norwegian Petroleum Directorate fact-pages of exploration wellbores. Available from:
<http://factpages.npd.no/factpages/Default.aspx?culture=en>. Date accessed: December, 2009.

Norwegian Petroleum Directorate, 2010a. The Norwegian Petroleum Directorate fact-pages of Goliat field. Available from:
<http://www.npd.no/engelsk/cwi/pbl/en/field/all/5774394.htm>. Date accessed: January, 2010.

Norwegian Petroleum Directorate, 2010b. The Norwegian Petroleum Directorate fact-pages of Snøhvit field. Available from:
<http://www.npd.no/engelsk/cwi/pbl/en/field/all/2053062.htm>. Date accessed: January, 2010.

Norwegian Petroleum Directorate, 2011. The Norwegian Petroleum Directorate:

Geological plays. Available from:

<http://www.npd.no/en/Topics/Geology/Geological-plays/>. Date accessed:

August, 2011.

Nøttvedt, A., Cecchi, M., Gjølberg, J.G., Kristensen, S.E., Lønøy, A., Rasmussen, A., Rasmussen, E., Skott, P.H., van Veen, P.M., 1993. Svalbard-Barents Sea correlation: a short review. In: Vorren, T.O., Bergsager, E., Dahl-Stammes, Ø.A., Holter, E., Johansen, B., Lie, E., Lund, T.B. (Eds.), Arctic Geology and Petroleum Potential. Norwegian Petroleum Society, Special Publication 2, pp. 363-375.

Nyland, B., Jensen, L.N., Skagen, J., Skarpnes, O., Vorren, T., 1992. Tertiary uplift and erosion in the Barents Sea: Magnitude, timing and consequences. In: Larsen, R.M., Brekke, H., Larsen, B.T., Talleraas, E. (Eds.), Structural and Tectonic Modelling and its Application to Petroleum Geology. Norwegian Petroleum Society, Special Publication, pp. 153-162.

O'Leary, N., White, N., Tull, S., Bashilov, V., Kuprin, V., Natavop, L., MacDonald, D., 2004. Evolution of the Timan-Pechora and South Barents Sea basins. Geological Magazine 141, 141-160.

Ohm, S.E., Karlsen, D.A., Austin, T.J.F., 2008. Geochemically driven exploration models in uplifted areas: Examples from the Norwegian Barents Sea. American Association of Petroleum Geologists Bulletin 92, 1191-1223.

Ostanin, I., Anka, Z., di Primio, R., Bernal, A., 2012. Identification of a large Upper Cretaceous polygonal fault network in the Hammerfest basin:

- Implications on the reactivation of regional faulting and gas leakage dynamics, SW Barents Sea. *Marine Geology* 332-334, 109-125.
- Ostanin, I., Anka, Z., di Primio, R., Bernal, A., 2013. Hydrocarbon plumbing systems above the Snøhvit gas field: structural control and implications for thermogenic methane leakage in the Hammerfest Basin, SW Barents Sea. *Marine and Petroleum Geology* 43, 127-146.
- Peters, K.E., Walters, C.C., Moldowan, J.M., 2005. *The Biomarker Guide. Biomarkers and Isotopes in Petroleum Exploration and Earth History.* Cambridge University, Cambridge, United Kingdom.
- Reemst, P., Cloetingh, S., Fanavoll, S., 1994. Tectonostratigraphic modelling of Cenozoic uplift and erosion in the south-western Barents Sea. *Marine and Petroleum Geology* 11, 478-490.
- Richardson, G., Knutsen, S.-M., Vail, P.R., Vorren, T.O., 1993. Mid-Late Miocene sedimentation on the southwestern Barents Shelf margin. In: Vorren, T.O., Bergsager, E., Dahl-Stamnes, Ø.A., Holter, E., Johansen, B., Lie, E., Lund, T.B. (Eds.), *Arctic Geology and Petroleum Potential.* Norwegian Petroleum Society, Special Publication, pp. 539-571.
- Riis, F., 1996. Quantification of Cenozoic vertical movements of Scandinavia by correlation of morphological surfaces with offshore data. *Global and Planetary Change* 12, 331-357.
- Riis, F., Fjeldskaar, W., 1992. On the magnitude of the Late Tertiary and Quaternary erosion and its significance for the uplift of Scandinavia and the

- Barents Sea. In: Larsen, R.M., Brekke, H., Larsen, B.T., Talleraas, E. (Eds.), Structural and Tectonic Modelling and its Application to Petroleum Geology. Norwegian Petroleum Society, Special Publication, pp. 163-185.
- Ritzmann, O., Faleide, J.I., 2009. The crust and mantle lithosphere in the Barents Sea/Kara Sea region. *Tectonophysics* 470, 89-104.
- Rodrigues Duran, E., di Primio, R., Anka, Z., Stoddart, D., Horsfield, B., 2013. 3D-basin modelling of the Hammerfest Basin (southwestern Barents Sea): A quantitative assessment of petroleum generation, migration and leakage, *Marine and Petroleum Geology*. *Marine and Petroleum Geology* 45, 281-303.
- Skagen, J.I., 1993. Effects on hydrocarbon potential caused by Tertiary uplift and erosion in the Barents Sea. In: Vorren, T.O., Bergsager, E., Dahl-Stamnes, Ø.A., Holter, E., Johansen, B., Lie, E., Lund, T.B. (Eds.), *Arctic Geology and Petroleum Potential*. Norwegian Petroleum Society, Special Publication 2, pp. 711-719.
- Thompson, K.F.M., 1983. Classification and thermal history of petroleum based on light hydrocarbons. *Geochimica et Cosmochimica Acta* 47, 303-316.
- Tissot, B., Welte, D., 1984. *Petroleum Formation and Occurrence*, Second Revised and Enlarged Edition, Springer-Verlag, Berlin, Heidelberg, New York, Tokyo.
- Vorren, T.O., Richardsen, G., Knutsen, S.-M., Henriksen, E., 1991. Cenozoic erosion and sedimentation in the western Barents Sea. *Marine and Petroleum Geology* 8, 317-340.

Weiss, H.M., Wilhelms, A., Mills, N., Scotchmer, J., Hall, P.B., Lind, K., Brekke, T., 2000. NIGOGA - The Norwegian Industry Guide to Organic Geochemical Analyses [online]. Edition 4.0 Published by Norsk Hydro, Statoil, Geolab Nor, SINTEF Petroleum Research and the Norwegian Petroleum Directorate. Available from: <http://www.npd.no/engelsk/nigoga/default.htm>.
Date accessed: June, 2013.

Whiticar, M.J., 1994. Correlation of natural gases with their sources. In: Magoon, L.B., Dow, W.G. (Eds.), *The Petroleum System - from Source to Trap*. American Association of Petroleum Geologists Memoirs.

Whiticar, M.J., 1996. Stable isotope geochemistry of coals, humic kerogens and related natural gases. *International Journal of Coal Geology* 32, 191-215.

Highlights

- Interpretation of basin modeling and organic geochemistry deconvolutes source and maturity.
- Gas analysis indicate maturity gradient from west to east.
- Light hydrocarbons support long range migration and biodegradation.
- Biomarkers indicate a contribution of two source rock facies types.
- Age related biomarkers did not allow a differentiation of the petroleum origin.

Figure captions

Figure 1 - The southwestern Barents Sea. The dashed square represents the area for which the Hammerfest Basin model was built (AFC: Asterias Fault Complex; BFC: Bjørnøyrenna Fault Complex; MFC: Måsøy Fault Complex; ND: Nordvarg Dome; NFC: Nyslepp Fault Complex; RLFC: Ringvassøy-Loppa Fault Complex; SD: Samson Dome; SvD: Svalis Dome; SLHFC: Southern Loppa High Fault Complex; TFFC: Troms-Finnmark Fault Complex).

Figure 2 - Lithostratigraphic chart for the Hammerfest Basin (adapted from Ohm et al., 2008). Potential source rocks (SR) and reservoirs (R) that have been proposed and found in the area, as well as the general overview of the geologic and tectonic history are shown.

Figure 3 - Bathymetry of the study area with wells distribution and 3D model view at present day. Notice the deeper western areas of the basin and the eastern shallower side with thinner sedimentary sequences. Calibration with well data in terms of vitrinite reflectance and temperature is also shown (for details regarding calibration, please refer to Rodrigues Duran et al., 2013). The list of wells shown in temperature calibration is the same for the VR calibration plots.

Figure 4 - Maturity level of the Hekkingen, Snadd and Kobbe formations. (a, c, e) Maturity maps in terms of vitrinite reflectance (VR) at present day, red lines in the maps represent the VR isolines. (b, d, f) Maturity history for six different pseudo-wells located in different areas of the Hammerfest Basin, especially where the maximum maturity level was reached and where the main fields and discoveries are located. The circles showed in “a” represent the six areas.

Figure 5 - Burial history of the main three source rocks considered in the model (Hekkingen, Snadd and Kobbe formations). Maximum burial depth was reached during Oligocene time (30 Ma), followed by the two main erosion events associated to tectonic uplift and glaciations.

Figure 6 – (a) Map of the main petroleum accumulations found in the Hammerfest Basin, which correspond to the Snøhvit, Albatross, Askeladd and Goliat fields and to the Tornerose discovery. Depth map of the main reservoir (Stø Formation) is used as the background. (b) Oil (green line) and gas (red line) filling history of the Stø Formation, the amounts are presented in mass units (Gt) and correspond to the sum of all hydrocarbon accumulations in this stratigraphic unit.

Figure 7 – (a, b, c, d, e) Migration pathways and drainage areas for the Askeladd, Albatross, Snøhvit, Goliat fields and the Tornerose discovery. The background shows the depth map of the Stø Formation. (f) Maturity map at present day of the Kobbe Formation (also shown in Fig. 5a) with the five drainage areas of each field and discovery.

Figure 8 - Oil and gas filling history of the Goliat field.

Figure 9 – (a) Correlation of gas-dryness ($C_1/(C_2 + C_3)$) with the methane isotopic composition. (b) Correlation of wetness percentage with the methane isotopic composition. Description of gas dryness and wetness percentage can be found in Section 6.2. The results for the Goliat field and the Tornerose discovery are shown in two areas corresponding to different stratigraphic levels, which are: the Tubåen, Snadd and Kobbe formations for the Goliat field, and the Stø and Snadd formations for the Tornerose discovery. The interpretation overlays stem from

p:IGI software and this correspond to an IGI synthesis of the references given in the software.

Figure 10 - Maturity interpretation using gas isotopic composition. The same separation of the results in relation to the stratigraphic levels and explained in Fig. 9 was used here. The interpretation overlays of this figure stem from p:IGI software as well.

Figure 11 - Light hydrocarbons (C7) oil correlation and oil transformation star diagrams (Halpern, 1995). The results for the Goliat field (yellow and pink lines) were taken from the work of Ohm et al. (2008). Oil correlation parameters correspond to: C1=2,2-dimethylpentane/P3; C2=2,3-dimethylpentane/P3; C3=2,4-dimethylpentane/P3; C4=3,3-dimethylpentane/P3; C5=3-ethylpentane/P3. Oil-transformation parameters correspond to: Tr1=toluene/1,1-dimethylcyclopentane; Tr2=*n*-C₇/1,1-dimethylcyclopentane; Tr3=3-methylhexane/1,1-dimethylcyclopentane; Tr4=2-methylhexane/1,1-dimethylcyclopentane; Tr5=P2/1,1-dimethylcyclopentane; Tr6=1*c*2-dimethylcyclopentane/1,1-dimethylcyclopentane; Tr7=1*t*3-dimethylcyclopentane/1,1-dimethylcyclopentane; Tr8=P2/P3. The P2 and P3 values correspond to: P2=(2-methylhexane+3-methylhexane); P3=(2,2-dimethylpentane+2,3-dimethylpentane+2,4-dimethylpentane+3,3-dimethylpentane+3-ethylpentane).

Figure 12 - Light hydrocarbons star diagrams using the Thompson (1983) interpretation. The different parameters correspond to: A=benzene/*n*-hexane; B=toluene/*n*-heptane; X=(*m*-xylene+*p*-xylene)/*n*-octane; C=(*n*-hexane+*n*-heptane)/(cyclohexane+methylcyclohexane); I=(2-+3-methylhexane)/(1*c*3+1*t*3+1*t*2-dimethylcyclopentanes); S=*n*-hexane/2,2-

dimethylbutane; F=*n*-heptane/methylcyclohexane; R=*n*-heptane/2-methylhexane; U=cyclohexane/methylcyclohexane.

Figure 13 - Correlation of the heptane and isoheptane ratios according to Thompson (1983). SLHFC = Southern Loppa High Fault Complex.

Figure 14 - Paleo-environment interpretation using: (a) Correlation of pristane/*n*-C₁₇ with phytane/*n*-C₁₈; (b) the C₂₇, C₂₈, C₂₉ steranes percentage; and (c) correlation of the dibenzothiophene/phenanthrene ratio with pristane/phytane ratio.

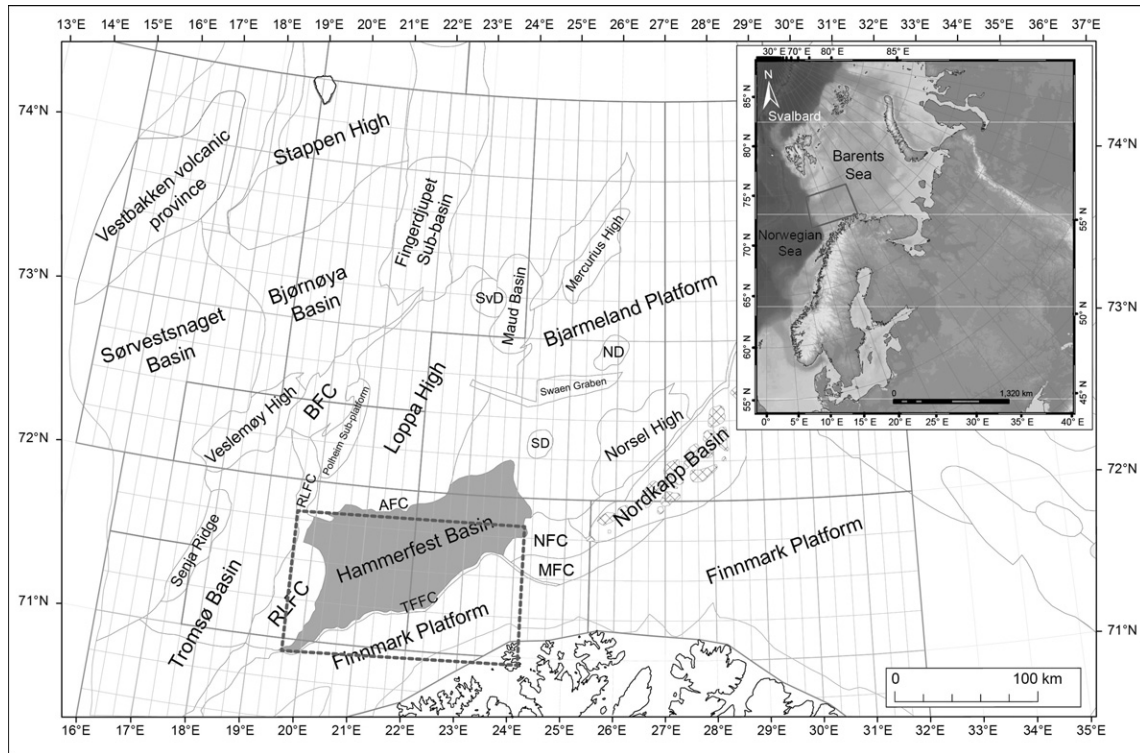
Figure 15 – (a, b, c, d, e) Maturity interpretation based on biomarkers using six ratios, which are: (1) C₃₂ 22S homohopane relative to C₃₂ 22R homohopane ratio; (2) 18 α 22,29,30 trisnorhopane (Ts) relative to 17 α 22,29,30 trisnorhopane (Tm); (3) C₂₇ diasteranes [13 β , 17 α (20S, 20R) diacholestanes and 13 α , 17 β (20S, 20R) diacholestanes] relative to C₂₉ steranes [5 α , 14 α , 17 α (20S, 20R) regular steranes and 5 α , 14 β , 17 β (20S, 20R) isosteranes] ratio; (4) isomerization index for C₂₉ regular steranes (5 α , 14 α , 17 α 20S regular steranes and 5 α , 14 α , 17 α 20R regular steranes); (5) racemization index for C₂₉ steranes or $\beta\beta/(\beta\beta+\alpha\alpha)$ ratio [5 α , 14 β , 17 β (20S, 20R) C₂₉ isosteranes relative to 5 α , 14 α , 17 α (20S, 20R) C₂₉ regular steranes], (6) mono-aromatic steroids ratio; and (7) tri-aromatic steroids ratio. (f)

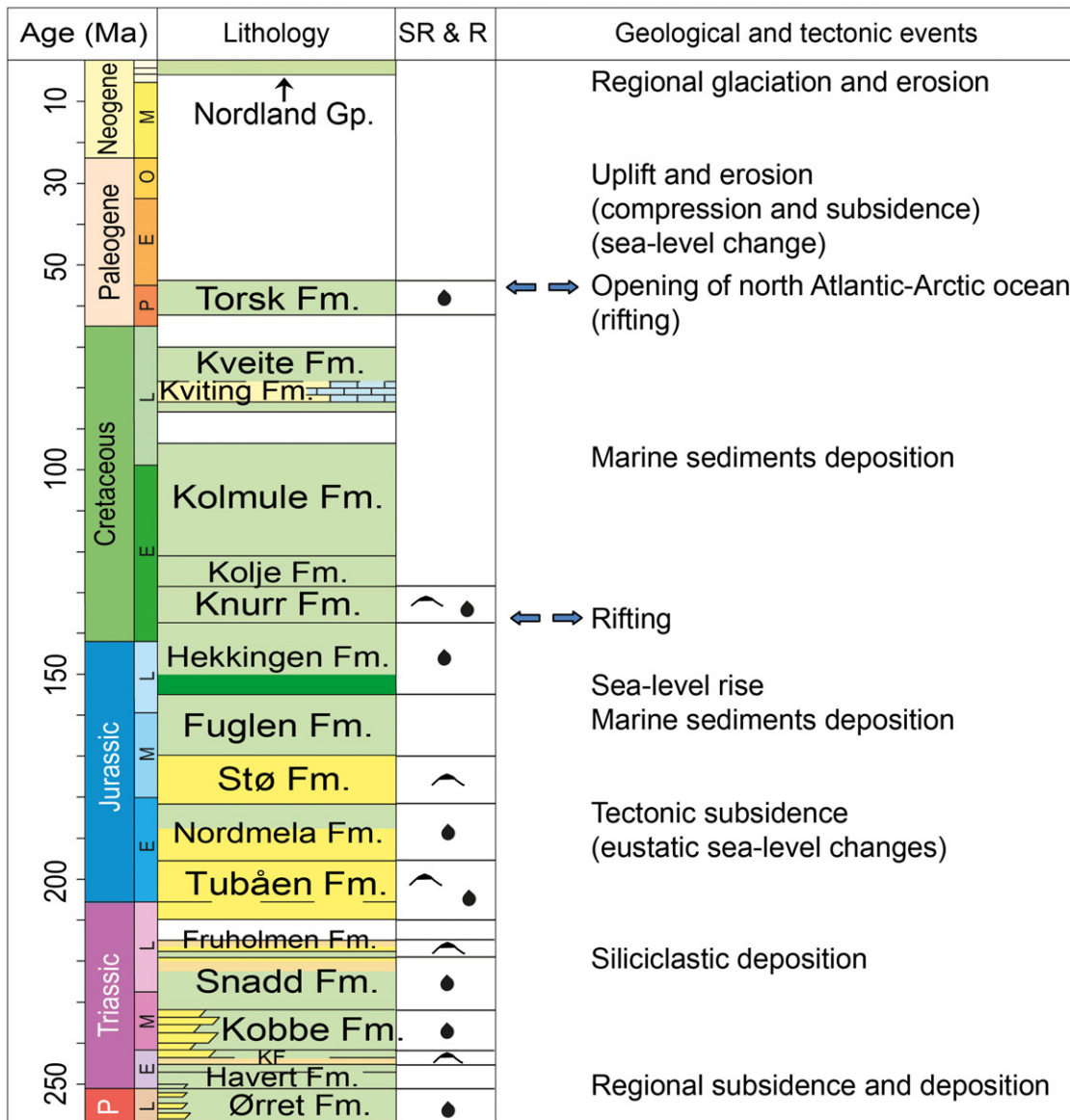
Approximate ranges of biomarker maturity ratios against vitrinite reflectance (Peters et al., 2005a). Here the terms west, east, northwest, northeast, central, Beta and North for the Albatross, Askeladd and Snøhvit fields are used. This nomenclature is based on the location of the samples as observed in the fields at the Norwegian Petroleum Directorate website (FactMaps).

Figure 16 - Correlation of the Ts/Tm and diasteranes/steranes ratios.

Figure 17 - Correlation of two age related biomarker ratios, the extended tricyclic terpane ratio (ETR) and the C₂₈/C₂₉ steranes ratio. SLHFC = Southern Loppa High Fault Complex.

ACCEPTED MANUSCRIPT





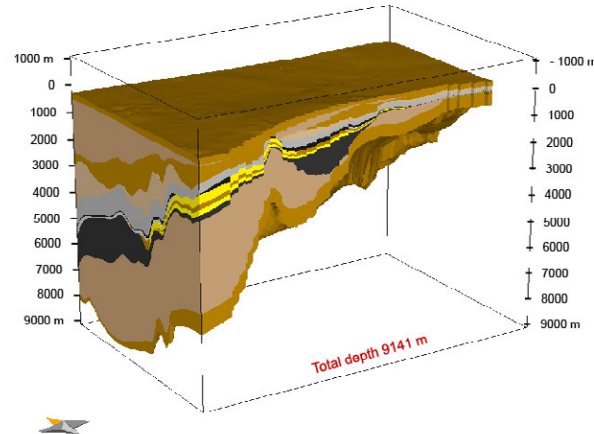
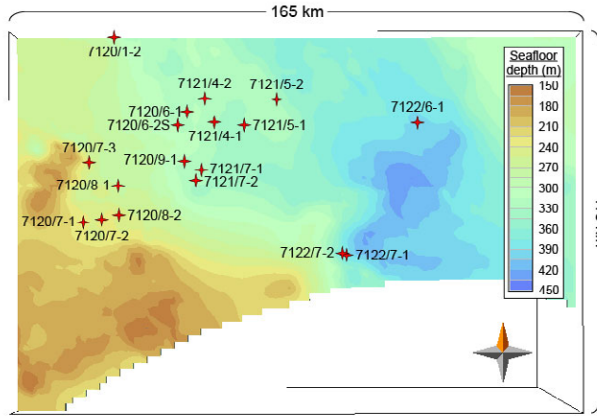
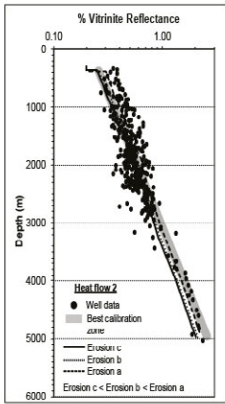
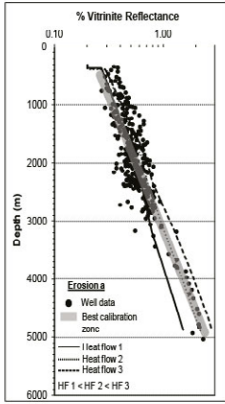
Organic-rich shale
 Marine shale
 Sandstone
 Alluvial shale

Limestone
 Estuarine
 Unconformity/Hiatus

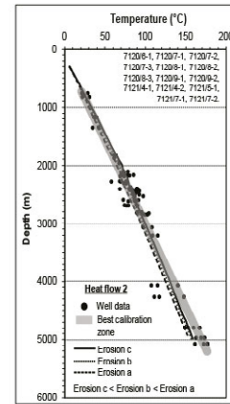
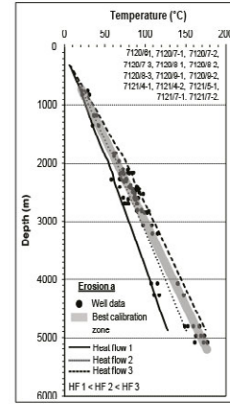
Extensional phase
 Source rock (SR)
 Reservoir (R)

AC

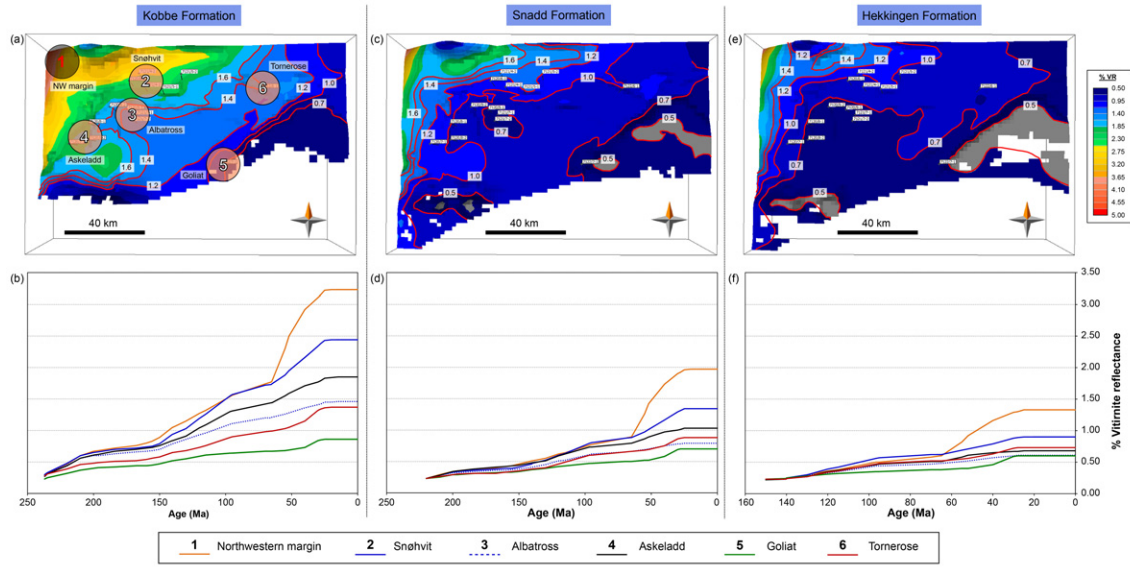
Vitrinite reflectance calibration

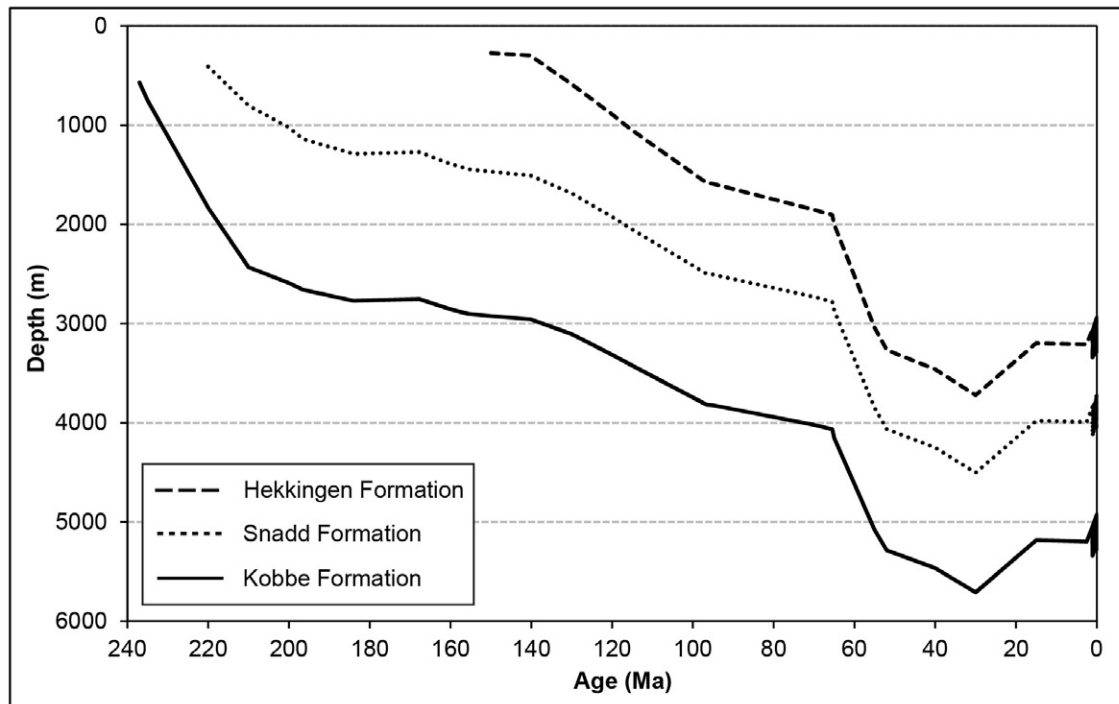


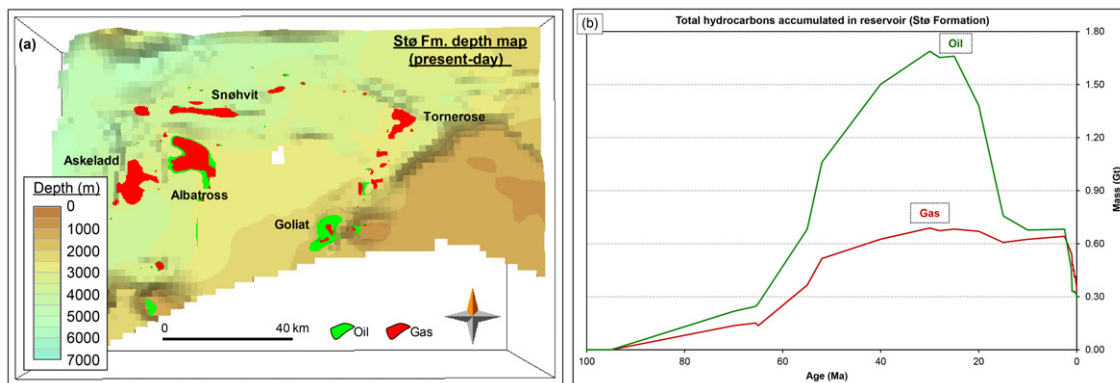
Temperature calibration

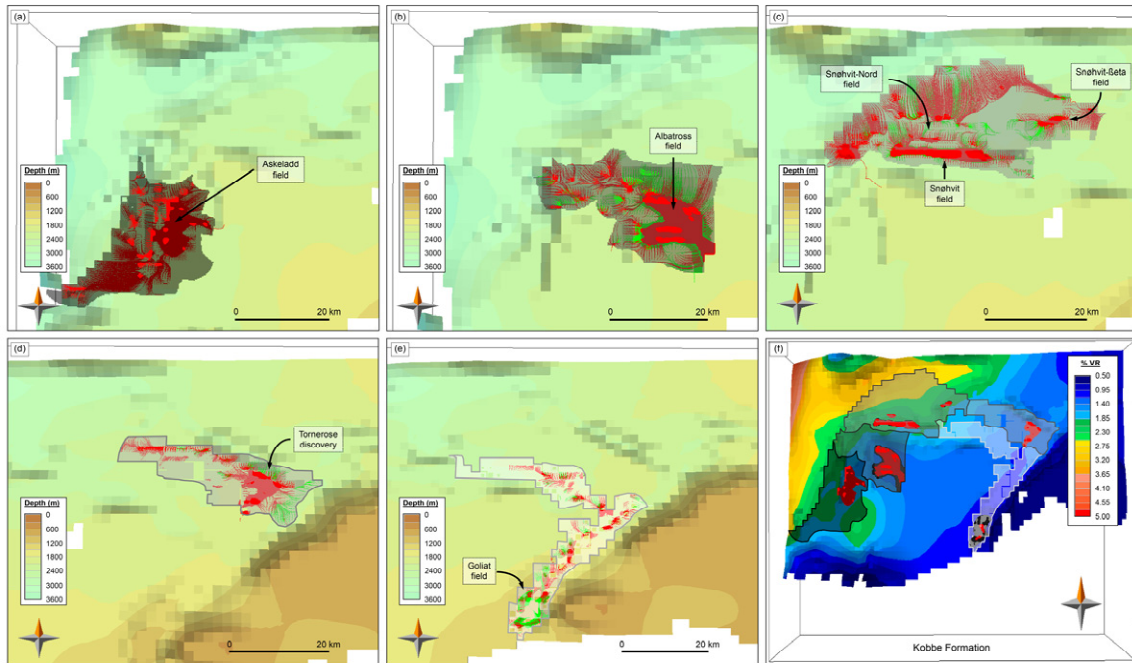


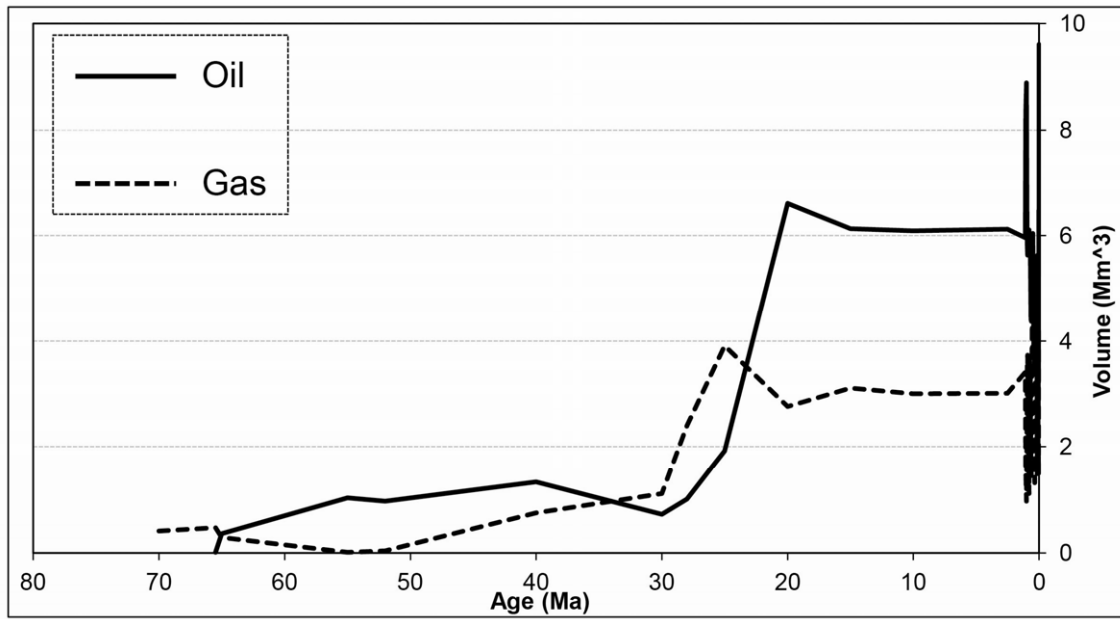
ACCEPTED

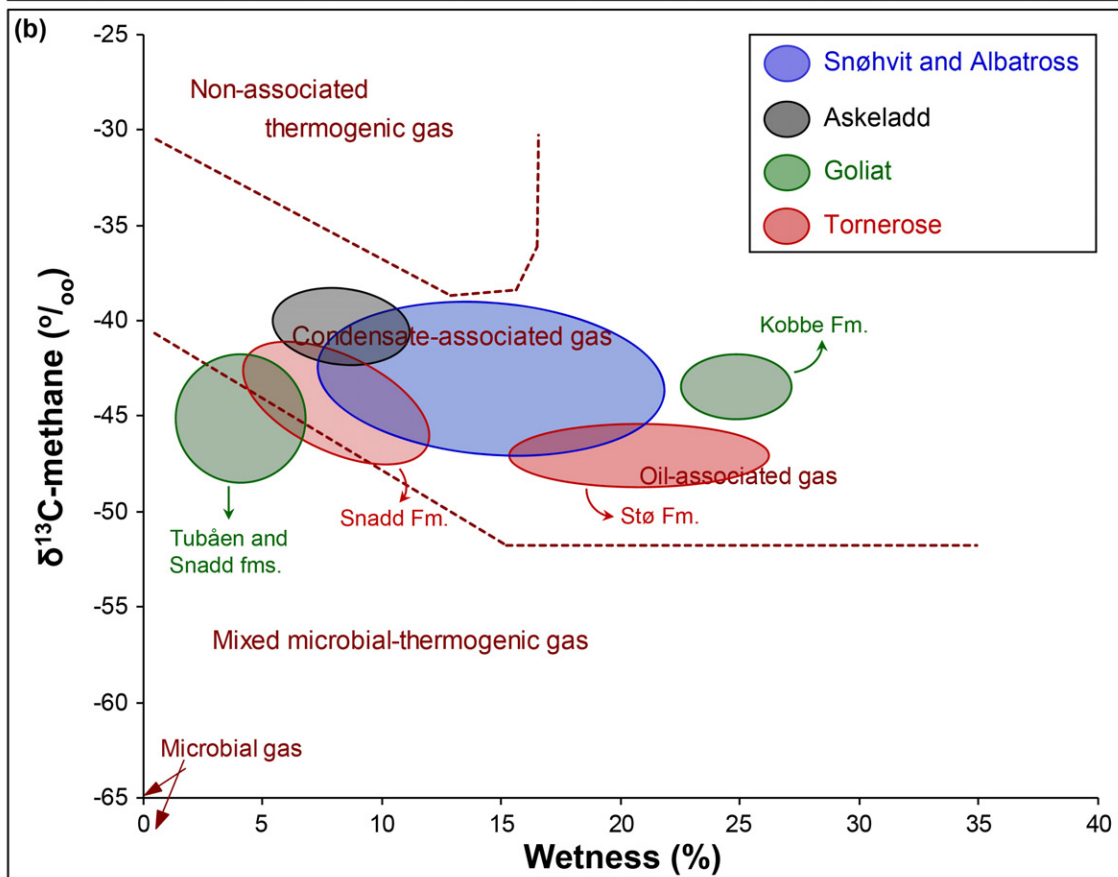
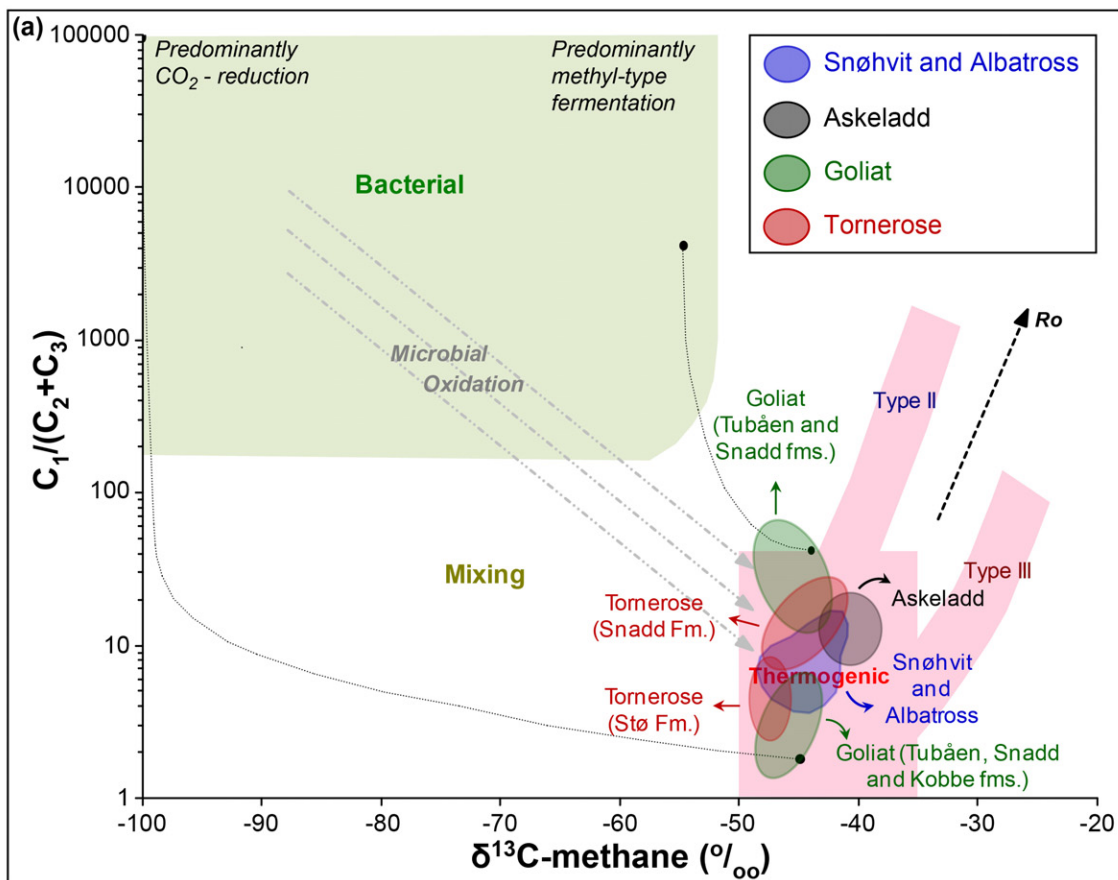


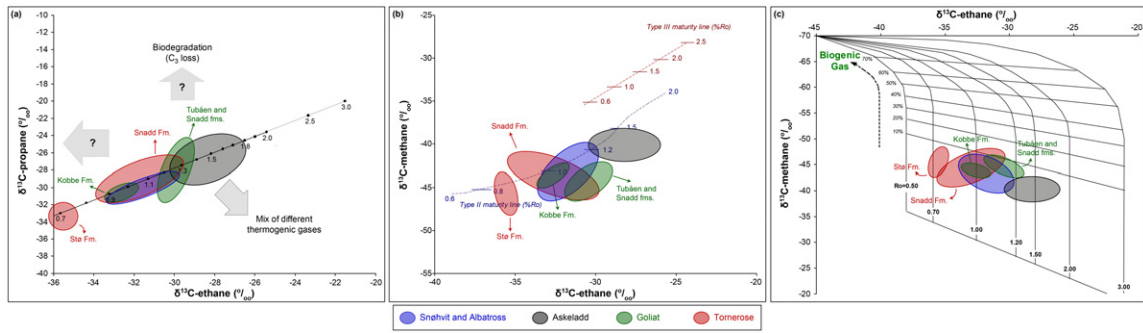




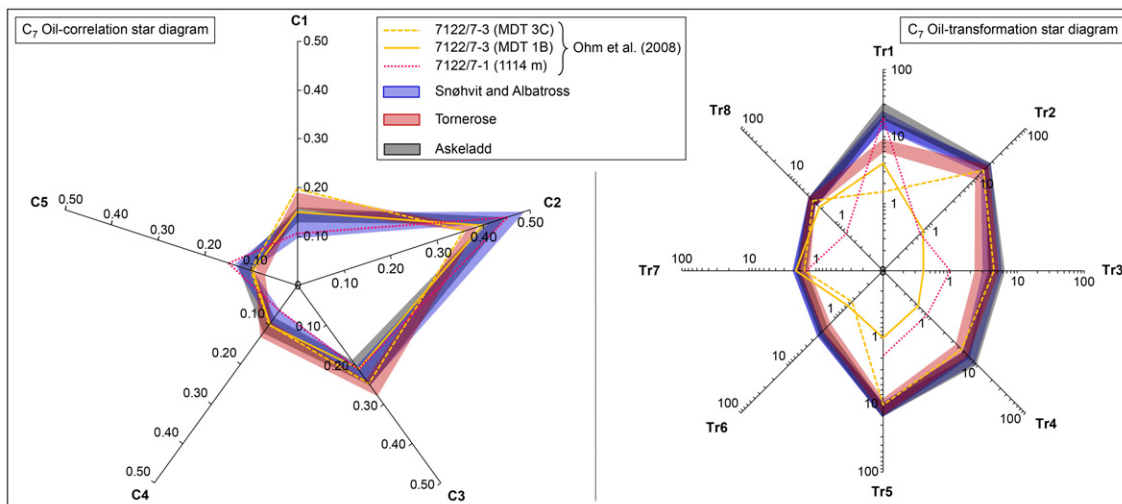




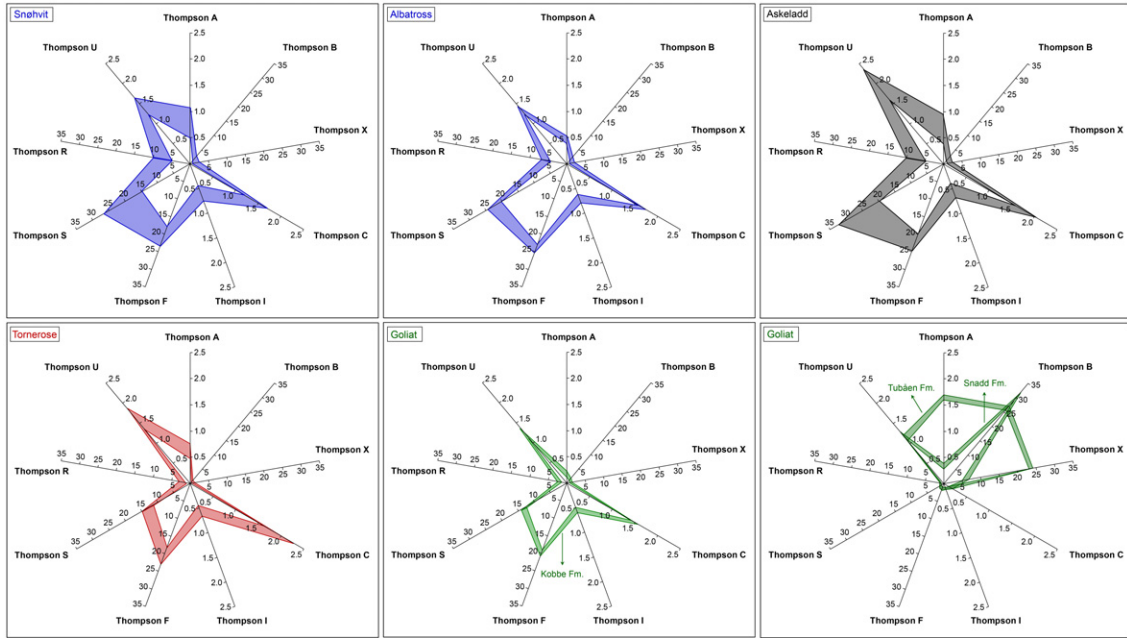




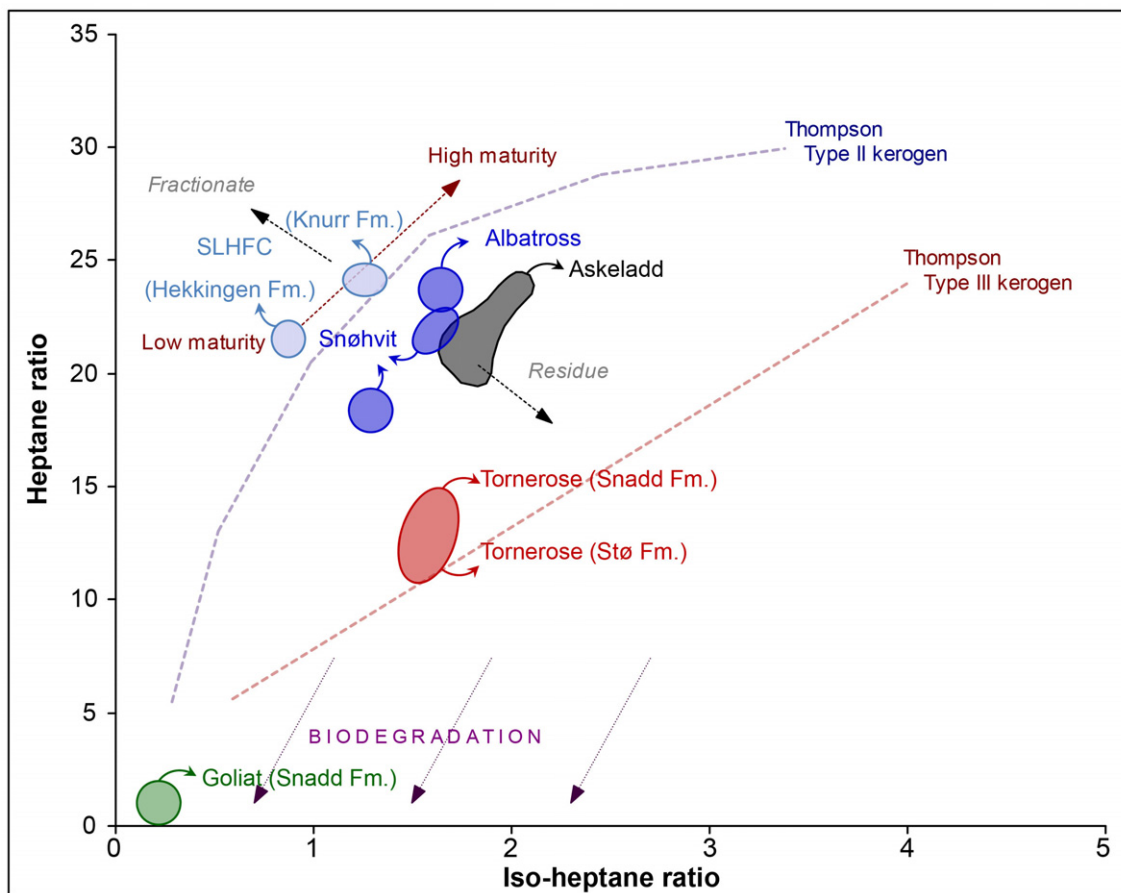
ACCEPTED MANUSCRIPT

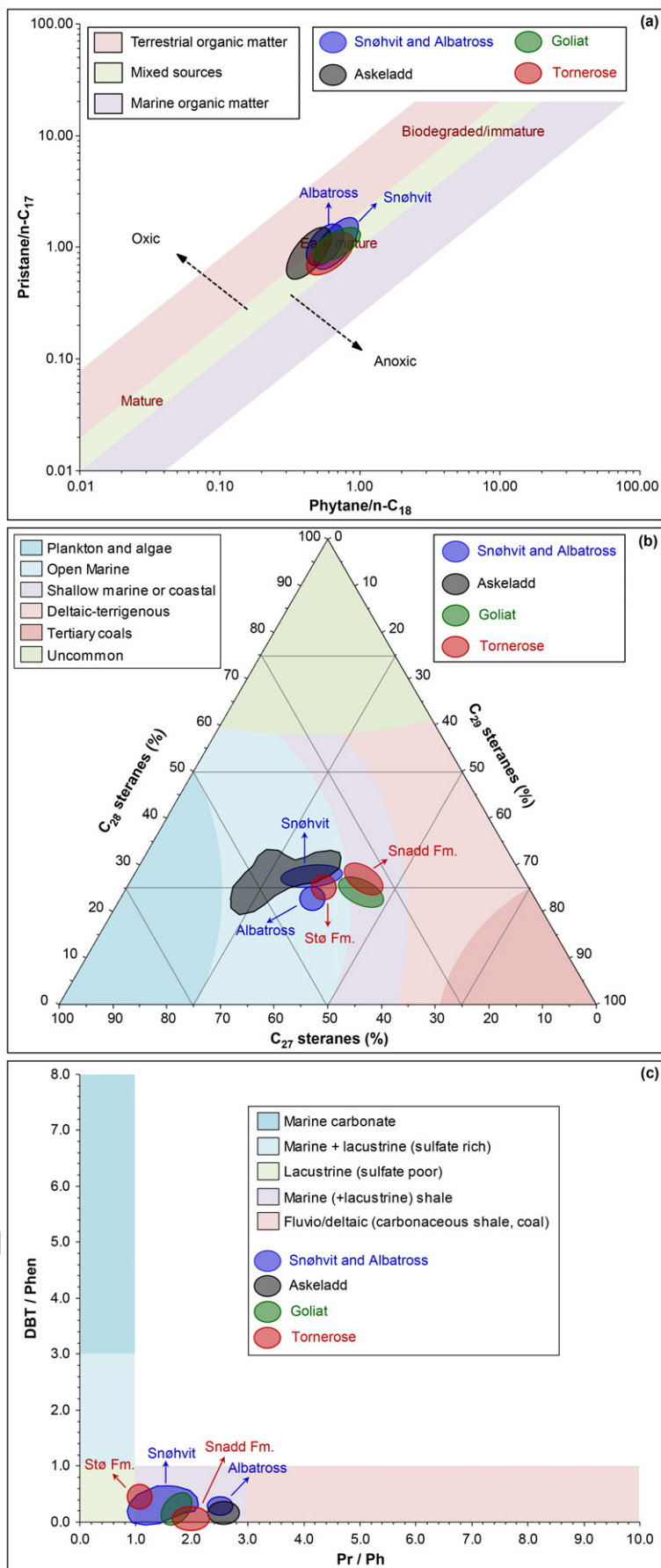


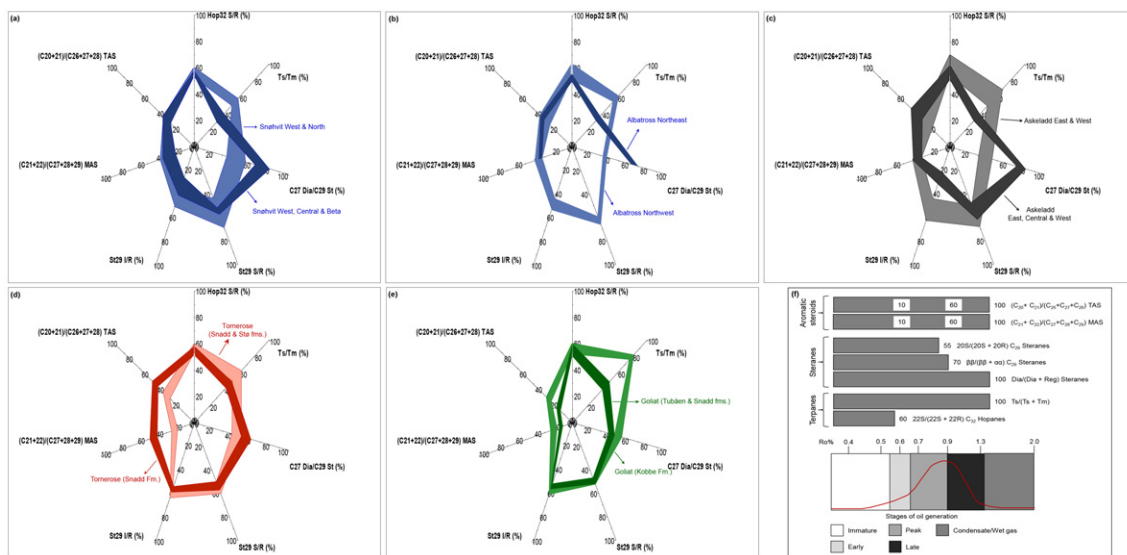
ACCEPTED MANUSCRIPT



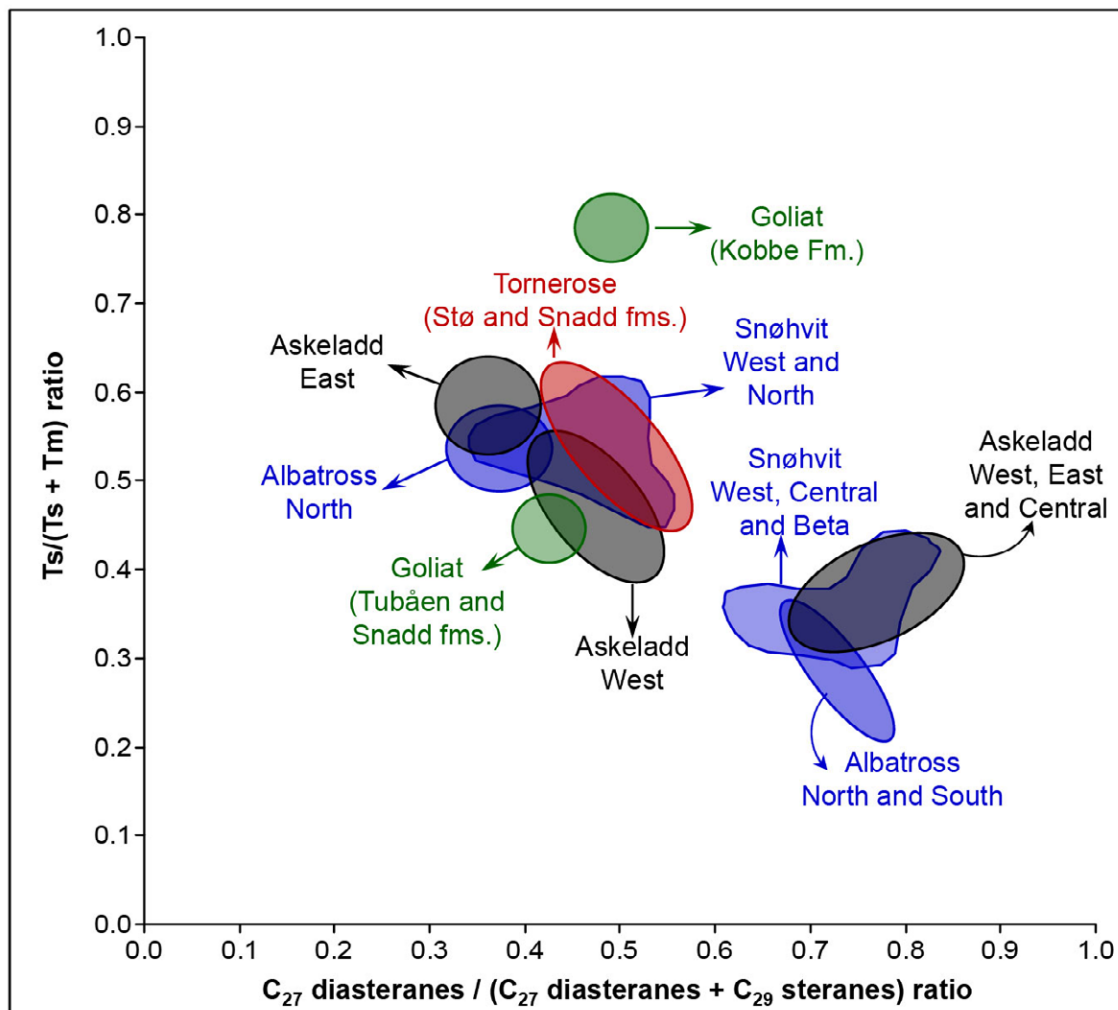
ACCEPTED MANUSCRIPT







ACCEPTED MANUSCRIPT



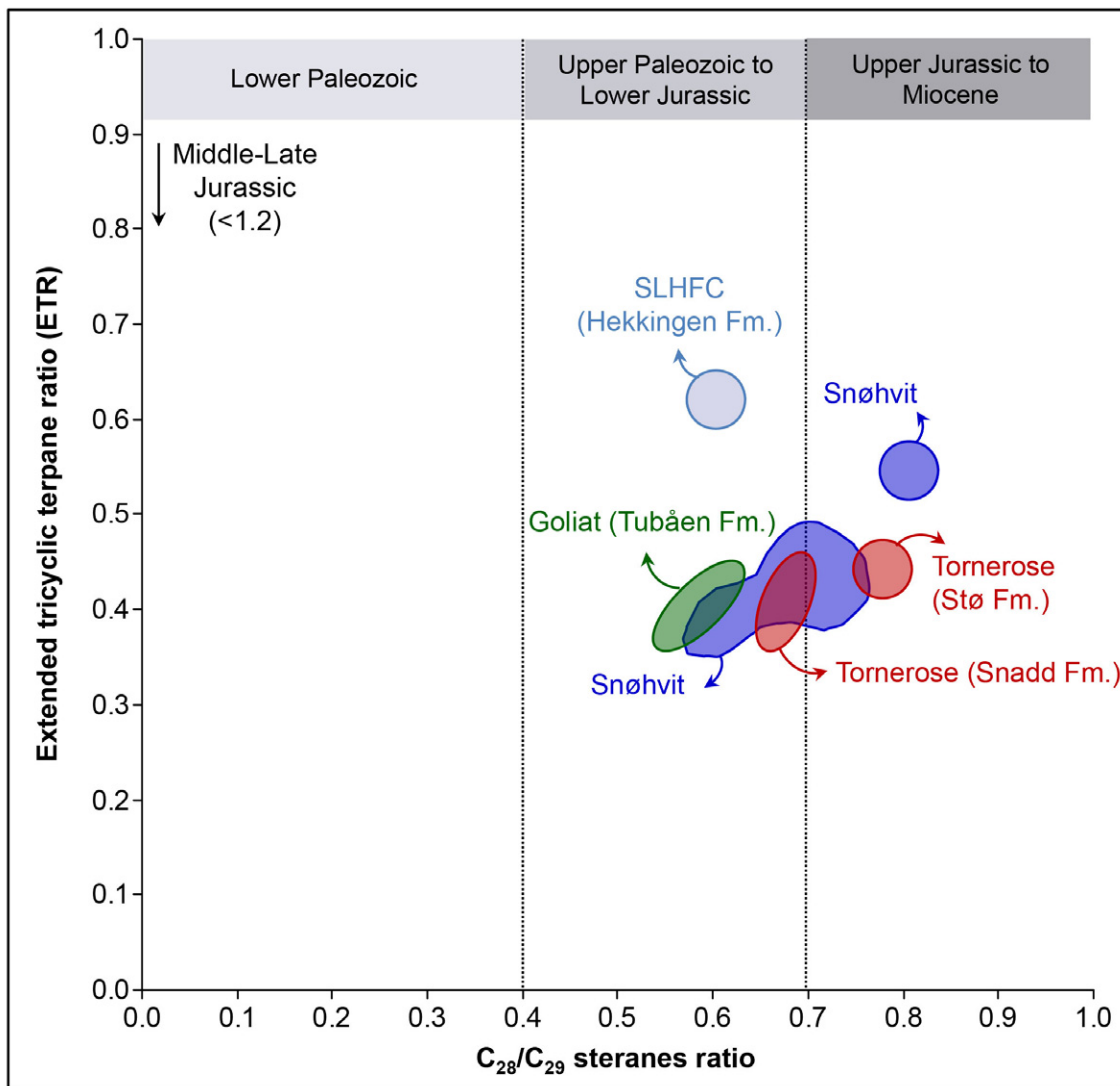


Table captions



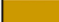



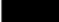
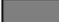




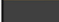





Table 1 - Petroleum plays description for the southwestern Barents Sea

Table 2 - Lithology definition input for PetroMod ®. Gp. = Group, Fm. = Formation, fms. = formations, PSE = Petroleum system elements, OR = Overburden rock, UR = Underburden rock, SR = Source rock, SeR = Seal rock, RR = Reservoir rock, TOC = Total organic carbon, HI = Hydrogen index, Soc = Critical oil saturation, Sgc = Critical gas saturation.

Table 3 - Description of the samples provided by Applied Petroleum Technology AS (Nr.: Number of samples; SLHFC: Southern Loppa High Fault Complex; HS: Headspace; Fm.: Formation; fms.: formations).

Table 4 - Contribution from each source rock to the main accumulations present in the Hammerfest Basin (mass %) based on results from the 3D basin model.

Name	Area	Reservoir rock	Source rock	Depositional environment	Trap	Fields/Discoveries
Paleocene – Supra Paleocene	Developed in the western area (Harstad Basin, Sarvestsnaget Basin and Vestbakken volcanic province)	Sandstone	Cretaceous shale (likely to be of poor quality and gas prone)	Shallow marine to moderately deep marine	Rotated fault blocks and stratigraphic pinch-out	Neither reservoir nor source rocks have been drilled so far.
Upper Jurassic to Lower Cretaceous	Limited distribution and restricted to paleo-highs in the western areas (southwestern flank of the Loppa High, the Senja Ridge-Veslemøy High, Finmark Platform)	Sandstone (deposited as lobes downflank from the highs)	Upper Jurassic Hekkingen Formation	Shallow to moderately deep marine	Stratigraphic pinch-out and occasionally fault dependent	Discovery in the well 7120/1-2
Lower to Middle Jurassic	Bjermøya, Hammerfest and Nordkapp Basins. Western part of the Bjarmeland Platform	Sandstones of Early to Middle Jurassic age	Upper Jurassic shales of the Hekkingen Fm. (major oil source). Lower Jurassic coals and carbonaceous shales (gas sources).	Fluvial, deltaic, estuarine tidal and shallow marine	Rotated fault blocks and horst structures	Snehvit, Albatross, Askeladd and Goliat fields. Tornerose, Nucula, Skrugard and Havis discoveries. Discoveries in wells 7120/12-2 and 12-3, 7124/3-1, 7125/1-1 7120/1 2, 7019/1-1 and 7119/12-3
Triassic	Bjermøya, Hammerfest and Nordkapp Basins. Bjarmeland and Finmark Platforms	Lower Triassic sandstones in the east. Lower, Middle and Upper Triassic sandstones in the west (Nordkapp Basin and eastern Hammerfest Basin)	Mainly relies on Triassic shales, Lower Carboniferous coal, Upper Permian shales and Lower Permian marls, all of them with a gas prone potential.	Fluvial, deltaic, shallow marine, tidal and estuarine	Stratigraphic (rotated fault blocks and halokinetic)	Goliat field. Tornerose, Nucula, Obesum and Veroveris discoveries. Discoveries in wells 7226/11-1, 7228/7-1, 7222/11-1, 7125/1-1, 7224/6-1 and 7223/5-1

Name	Structural map used to define the stratigraphic level	Color scale	PSE	TOC (%)	HI (mgHC/gTOC)	Lithology
Nordland Gp.	Seabed		OR			Siltstone (organic lean)
Torsk Fm.	Base Quaternary		OR			Shale (organic lean, typical)
Kveite-Kviting fms.	Top Kveite		OR			Siltstone (organic lean)
Kolmule Fm.	Top Kolmule		OR			Shale (organic lean, silty)
Kolje Fm.	Top Kolje		OR			Shale (typical)
Knurr Fm.	Top Knurr		OR			Shale (typical)
Hekkingen Fm.	Top Hekkingen		SR	10	300	Shale (organic rich, 8% TOC) Soc=Sgc
Fuglen Fm.	Base Hekkingen		SeR			Shale (organic lean, siliceous, typical)
Stø Fm. 01	Top Stø		RR			Sandstone (typical)
Stø Fm. 02	Top Stø		OR			Siltstone (organic lean)
Nordmela Fm.	Base Stø		OR			Siltstone (organic lean)
Tubåen Fm.	Base Stø		RR			Sandstone (clay poor)
Fruholmen Fm.	Base Stø		OR			Siltstone (organic rich, 2-3% TOC)
Snadd Fm.	Top Snadd		SR	2	150	Siltstone (organic rich, 2-3% TOC) Soc=Sgc
Kobbe Fm.	Top Kobbe		SR	3	200	Siltstone (organic rich, 2-3% TOC) Soc=Sgc
Havert-Klappmys fms.	Base Kobbe		UR			Shale (organic lean, silty)
Ørret Fm.	Top Ørret		UR			Siltstone (organic lean)
Basement	Base Ørret		UR			Basement

Sample	Nr.	Field/Discovery	Stratigraphic level
Oil	4	Snøhvit	Stø Fm.
	1	Albatross	Stø Fm.
	8	Goliat	Tubåen, Snadd and Kobbe fms.
	1	Tornerose	Stø Fm.
	3	7120/1-2 (SLHFC)	Hekkingen and Knurr fms.
Oil/Condensate	2	Askeladd	Stø Fm.
Condensate	3	Snøhvit	Stø and Tubåen fms.
	1	Albatross	Stø Fm.
	4	Askeladd	Stø Fm.
	1	Tornerose	Snadd Fm.
Oil/Gas	3	Tornerose	Snadd Fm.
Gas	4	Snøhvit	Stø Fm.
	13	Tornerose	Stø and Snadd fms.
HS Gas	5	Snøhvit	Stø and Tubåen fms.

Age	Source rock	Snøhvit		Albatross		Askeladd	Goliat		Tornerose
		Vapor	Liquid	Vapor	Liquid	Vapor	Vapor	Liquid	Vapor
Jurassic	Hekkingen Fm.	43	69	25	28	18	24	18	30
Triassic	Snadd Fm.	29	22	44	49	49	45	52	26
Triassic	Kobbe Fm.	28	9	31	23	33	31	30	44

ACCEPTED MANUSCRIPT